

Review

Sand and Dust Storms' Impact on the Efficiency of the Photovoltaic Modules Installed in Baghdad: A Review Study with an Empirical Investigation

Miqdam T. Chaichan ¹, Hussein A. Kazem ², Ali H. A. Al-Waeli ³, Kamaruzzaman Sopian ⁴, Mohammed A. Fayad ¹, Wissam H. Alawee ⁵, Hayder A. Dhahad ⁶, Wan Nor Roslam Wan Isahak ⁷ and Ahmed A. Al-Amiery ^{1,7,*}

¹ Energy and Renewable Energies Technology Center, University of Technology, Baghdad 10001, Iraq

² Faculty of Engineering, Sohar University, P.O. Box 44, Sohar 311, Oman

³ Engineering Department, American University of Iraq, Sulaymaniyah 46001, Iraq

⁴ Department of Mechanical Engineering, Universiti Teknologi PETRONAS, Seri Iskandar 32610, Perak Darul Ridzuan, Malaysia

⁵ Control and Systems Engineering Department, University of Technology, Baghdad 19006, Iraq

⁶ Mechanical Engineering Department, University of Technology, Baghdad 10066, Iraq

⁷ Department of Chemical and Process Engineering, Faculty of Engineering and Built Environment, Universiti Kebangsaan Malaysia (UKM), Bangi 43000, Selangor, Malaysia

* Correspondence: dr.ahmed1975@gmail.com or dr.ahmed1975@ukm.edu.my

Abstract: Airborne dust and dust storms are natural disasters that transport dust over long distances from the source basin, sometimes reaching hundreds of kilometers. Today, Iraq is a basin that produces dust storms that strike all neighboring countries such as Iran, Kuwait and Saudi Arabia. These storms affect the productivity and capacity of the photovoltaic modules and reduce the amount of electricity that is generated clearly. Airborne dust reduces the intensity of solar radiation by scattering and absorbing it. In addition, the dust accumulated on the photovoltaic modules causes a deterioration in their productivity. In this study, an extensive review of wind movement and its sources, especially those that hit the city of Baghdad, the capital of Iraq, was conducted. Practical experiments were also carried out during a storm to measure important variables that had not been measured practically before at this site. The experimental tests were carried out starting from 1 April 2022 and continued until 12 April. Within this period, a dust storm occurred that lasted for three consecutive days that was considered one of the most severe storms that the city of Baghdad had experienced in the last few years. Practical measurements showed a deterioration in the solar radiation intensity by up to 54.5% compared to previous days. The air temperature during the storm decreased by 21.09% compared to the days before the storm. From the measurements of ultrafine aerosol particles PM1 and PM2.5, there was a significant increase of 569.9% and 441% compared to the days before the storm, respectively. Additionally, the measurements showed an increase of 217.22% and 319.21% in PM10 and total suspended particles, respectively. Indoor performance experiments showed a deterioration of current, voltage, power and electrical efficiency by 32.28%, 14.45%, 38.52% and 65.58%, respectively, due to dust accumulated during the storm days compared to the previous days. In the outdoor experiments, the rates of deterioration of current, voltage, power and electrical efficiency were greater, reaching 60.24%, 30.7%, 62.3% and 82.93%, respectively, during the storm days compared to the days before it. During a storm, cleaning the panels is futile due to the high concentration of dust in the air, especially by water. However, the photovoltaic modules can be dry cleaned with bristle brushes after the storm has subsided.

Keywords: sand and dust storms; PM1.0; PM2.5; total suspended particles; photovoltaic modules performance



Citation: Chaichan, M.T.; Kazem, H.A.; Al-Waeli, A.H.A.; Sopian, K.; Fayad, M.A.; Alawee, W.H.; Dhahad, H.A.; Isahak, W.N.R.W.; Al-Amiery, A.A. Sand and Dust Storms' Impact on the Efficiency of the Photovoltaic Modules Installed in Baghdad: A Review Study with an Empirical Investigation. *Energies* **2023**, *16*, 3938. <https://doi.org/10.3390/en16093938>

Academic Editor: Alessandro Massi Pavan

Received: 4 December 2022

Revised: 29 December 2022

Accepted: 16 January 2023

Published: 7 May 2023



Copyright: © 2023 by the authors. Licensee MDPI, Basel, Switzerland. This article is an open access article distributed under the terms and conditions of the Creative Commons Attribution (CC BY) license (<https://creativecommons.org/licenses/by/4.0/>).

1. Introduction

Since the end of the last century, there has been interest in exploiting solar energy to generate electricity as it is clean, free and available most days of the year. Improvements in the efficiency of photovoltaic (PV) modules and their high productivity has caused an increase in the spread and expansion of their use. Today, PV electricity generation is the most competitive option in many locations around the world. Böök & Lindfors (2020) demonstrated the increase in the exploitation of solar energy and the escalation in the growth of PV systems in recent years [1]. By the end of 2019, the electrical capacity generated using PV systems amounted to approximately 2.8% of the total electricity generated globally. There are many PV stations installed in Europe and the United States and new markets have emerged, but with increasing demand, such as countries in the Middle East and Africa. For example, the United Arab Emirates, the Kingdom of Saudi Arabia and Oman have shown an interest in the exploitation of solar energy and the installation of PV modules in the Middle East [2].

The greatest challenge facing solar PV plants is that these technologies are subject to weather conditions, which affect their performance. Practically, achieving a balance between supply and demand (especially during peak hours) is one of the most important basics of electric power production so that the station can schedule energy production. In PV plants, production scheduling is an exceedingly challenging task compared to fossil fuel plants due to weather factors [1,3]. The most important weather variables that directly affect PV modules are the intensity of solar radiation, temperature, relative humidity and dust. In addition, the performance of any photovoltaic system is affected by a variety of external conditions. The most important of these conditions are hot spots, partial shade and other minor malfunctions [4,5]. The effect of dust on PV modules is significant as it reduces the solar radiation intensity reaching the PV module and, in turn, its productivity. Dust accumulation also prevents a large part of the irradiance from reaching the surfaces of PV modules. To eliminate traces of dust, the researchers unanimously agreed on the necessity of periodic cleaning of the PV modules, either monthly or weekly, depending on the weather conditions and the amount of dust suspended in the air. For example, Ramli et al. (2016) found that PV modules should be cleaned every two weeks in high-humidity climates [6]. In Jordan, Hammad et al. (2018) suggest periodic cleaning of photovoltaic cells every 12 to 15 days depending on the type of PV module [7]. Chaichan et al. (2015) suggested that dust containing a high percentage of carbon particles be cleaned using a sodium solution to achieve a higher cleaning efficiency than cleaning with alcohol. The authors also concluded that PV modules installed near highways in Baghdad should be cleaned every 10 days [8].

Dust storms are common and the Baghdadi citizen may have become accustomed to them due to the recurrences over the last three decades. At the Nairobi Conference on 12 February 2013, the representative of the Secretary-General of the United Nations, Martin Kobler, stated that Iraq had faced approximately 122 sand and dust storms during the year 2012 and the years that preceded it. He expected that this country would face up to 300 dust storms annually during the coming 5 years [9]. In 2012, the Iraqi Ministry of Environment supported this information; its reports mentioned the occurrence of 122 dust storms and 283 dusty days and concluded that Iraq might witness more than 300 dust days and dust storms over the next 10 years [10]. In the year 2022, the United Nations and the Iraqi Ministry of Environment announced that Iraq had been exposed to a large number of dust storms [11] that had resulted in the death of many citizens due to suffocation, with more than 5000 citizens being transferred to hospitals for treatment [12]. Additionally, the government stopped air flights from Baghdad and Najaf airports [13,14]. The orange color of the sky associated with low levels of visibility has become common in Iraq [15]. Figure 1 shows pictures of citizens suffering from dust storms. The “Iraqi Meteorological Office” has predicted dangerous occurrences, the most important of which is that the phenomenon of dust storms will increase as a direct result of the drought that has been ongoing for four decades, desertification and reduced rainfall [16]. In April 2022, seven dust storms occurred

that were categorized as severe to medium. The dust storms caused almost complete disruption of daily life in Baghdad Governorate [17].



Figure 1. Dust storms in Baghdad and the suffering of citizens during these storms.

This study is concerned with the impact of dust and dust storms on PV power stations and modules. The Iraqi Ministry of Electricity expects that 15% of the electricity produced by 2030 will be from photovoltaic power plants. Therefore, the frequency of these storms and their devastating effects on the productivity of photovoltaic modules is an important matter that must be investigated and measured. The results of this study, along with the review that precedes it, can establish a solid basis for making decisions related to the location of PV power stations in Baghdad Governorate and the rest of Iraq, the economic feasibility of these stations, and their long-term operational success in providing stable electricity. With the advancement of meteorology and its use of satellites to predict such storms, there is still interest in how to neutralize these storms or at least reduce their effects on the productivity of photovoltaic plants. This study is divided into several sections after the introduction. In the second section, a detailed study of dust and winds and their formation, causes and results are presented. The third section discusses dusty winds in Baghdad, their causes and consequences. The fourth section elucidates the effect of dust on PV modules. The fifth section presents practical measurements of dust storms that passed through Baghdad in April 2022. The sixth section discusses the results. The paper then offers conclusions and recommendations for future work.

2. Dust Storms: Formation, Causes and Results

2.1. Dusty Winds: Causes and Consequences

Dust storms form when air moves at high speed, creating strong winds that can lift and move dust particles and surface soil sands and transport them over long distances. With the increase in the density of dust and sand transmitted through the air, these moving particles over sand or loose soil perform the process of sculpting and shaking the soil particles, disintegrating them and then moving them across the surface. As the tiny dust particles in the soil loosen and break, they begin to rise and move in the air. These particles, in turn, encounter the surface of the soil, causing more of its particles to disintegrate, which then begin to rub against other particles, doubling the number of dust and sand particles that move with the wind.

The main factors that cause the disintegration of sand/dust particles and facilitate the process of their rise and movement with the wind and the formation of sand and dust storms are as follows:

1. Drying of the soil for extended periods of time extending to dozens of years.
2. A lack of rain and absence of vegetation.
3. Air movement at high-speed, creating high winds.
4. Wrongful human practices, such as intensive plowing of dry lands and overgrazing.
5. The movement of wheels and vehicles in arid lands, which crumbles and disintegrates the soil.

Dust storms represent an environmental hazard and are frequent in arid and semi-arid regions of the world [18]. Sand and dust storms constitute natural disasters that have devastating effects on the environment and human health. The Middle East and North Africa (MENA) region can be considered the world's largest natural source of dust, with dust and dust storms accounting for more than half of the average annual global dust emissions [19]. Huneus et al. (2011) determined the global dust emission rate to be approximately 500–4000 Tg/yr; the share of North Africa and the Middle East is 400–2200 Tg/yr and 26–526 Tg/yr, respectively [20]. China also represents one of the epicenters of dust storms in Central Asia [21]. Excessive amounts of dust illustrate the environmental effects of the region as shrinkage and atmospheric erosion play a significant role in creating conditions suitable for dust generation [22]. This affects local, regional and global climate systems which are in turn influenced by environmental and atmospheric variables. Dust affects the climate, however, there is an influence of the climate on the rise of dust, its volatilization over long distances and its precipitation. The researchers noticed in this issue the interdependence of these two variables, as any change in the climate due to dust results in a clear change in the rate of dust generation, escalation and transportation in the atmosphere. It is difficult to monitor dust storms effectively in the Middle East and North Africa region because of the limitation of satellite and spectrophotometer monitoring due to the large area of this region.

Reports by the “Intergovernmental Panel on Climate Change” (IPCC) in 2021 showed that the negative effects of global warming such as dust storms, strong convection systems, hot temperatures and heat waves are becoming more frequent. Wang et al. (2021) defined a dust storm as an extreme atmospheric phenomenon that affects the global climate [23], as defined by Luo (2010) [24]. It is a climatic phenomenon caused by intense winds that uproot, volatilize, and transport dust and sand from the surface of the earth to great distances. Dusty and sandy winds cause a decrease in horizontal visibility to less than 1 km. These winds carry serious dangers as they destroy the environment and endanger human health, impeding the economic development of the countries they pass through [25]. Gu et al. (2021) explained that dust storms formed due to three basic factors: high air speed (intense winds), availability of a sand/dust source and unstable weather conditions (atmospheric depressions and heights) [26]. Sand and dust storms occur in arid and semi-arid regions of North America, Australia, Central Asia, the Middle East and the Sahara Desert [23,27].

2.2. Negative Effects of Dust Storms

Luo et al. (2004) showed that dust storms (during the storm and the days after it) contain a large variety of particulate matter pollutants [28]. Thus, most researchers consider these storms to be a major cause of air pollution. Zhang et al. (2003) estimated that the proportion of mineral dust aerosols may range from 45% to 82% during a dust storm [29]. Processes such as adsorption, catalysis and heterogeneous interactions of volatile organic compounds (VOCs) on the surface of a mineral dust aerosol can cause a phase change in atmospheric gases and particulate matter [29]. Such variability can significantly affect climate change and the atmospheric environment [30,31]. Dust storms can also reduce light intensity; Zhao et al. (2011) showed that the direct radiative effect of aerosols occurs via the scattering and absorption of incoming solar radiation and outgoing terrestrial radiation [32]. Garland et al. (2009) clarified that the aerosol dispersion coefficient in

the case of a dust storm is approximately 5–10 times higher than the aerosol absorption coefficients in different locations in Beijing for the period from 1999 to 2009 [33]. These storms cause a deterioration in the productivity of PV modules due to the attenuation of solar radiation and the increase in dust accumulation on these modules [34,35].

Dust storms cause soil fertility degradation due to biogeochemical processes that increase the growth of marine phytoplankton when they are deposited on land and in oceans. As a result of this, the global carbon cycle is affected [36,37]. These storms cause an obstacle to the irradiance, which causes a decrease in air and surface temperature with soil loss, which results in negative effects on agricultural production and plant growth [38].

In general, these storms affect air quality and increase mortality rates related to respiratory and cardiovascular diseases [39] and also reduce horizontal visibility, which increases traffic accidents and the number of victims of these accidents [40].

3. Dust Storms in Iraq

Since the beginning of the current century until today, the frequency of sand and dust storms has been increasing in Iraq. This country is exposed to continuous drought and interruption of precipitation, which causes desertification and a decrease in vegetation cover. Global warming has played a significant role in the circumstances that Iraq currently suffers from. Zoljoodi (2013) stated that the period from 2001 to 2012 was the warmest in the past four decades [41]. Since 2012, the occurrence of drought has been increasing and has caused the expansion of arid regions and desertification at the expense of green areas [42].

Iraq is located at the center of what is called the global dust belt, which extends from the Sahara Desert across the Middle East to the Gobi Desert in Mongolia and China [43]. This belt contains permanent dust sources (arid deserts). A large part of Iraq is a desert area and an increasing part of the country is subject to desertification [44]. Surface wind movement causes the release of millions of tons of dust that negatively affects human life [45], increases road accidents and deteriorates solar radiation intensity [46,47]. The global dust belt contains Earth's most famous deserts, such as the Great Sahara, the Empty Quarter, the desert of western Iraq and the Levant, which were formed hundreds of years ago due to a lack of rain and elevated temperatures. When these areas are exposed to winds, strong dust storms arise that reduce horizontal visibility to 5 km and sometimes less than 100 m [48]. The severe and prolonged drought that has afflicted the "West Asian" region over the past two decades has caused an increase in dusty winds and the amount of soil, sand and dust suspended in the atmosphere in this region. Kazem et al. (2022) demonstrated that the transformation of a large part of the Fertile Crescent into barren lands and deserts made Mesopotamia a basin for the production and export of dust, the effects of which reach all the countries surrounding Iraq [49].

Baghdad city, the capital of Iraq, is situated in a flat, moderate and dry plain area with little or no vegetation cover. The flatness of the earth extends to vast distances of barren lands with loose soil. Baghdad is surrounded by terrain consisting of highlands to the east and north, plateaus to the west, and flat lands to the south. This topography makes the province of Baghdad a meeting place for centers of atmospheric pressure [50]. The fast winds that pass through these dry lands disturb the dry soil and break the bonds between the dust particles and force them to move. Particles attached to the surface cannot move and rise in a vacuum and then move without the presence of an external factor that is stronger than their adhesion and weight and that can lift these particles and transport them over long distances [51]. One of the most important conditions for the occurrence of dust storms is that the wind speed is not less than 25 km/h. The frequency of such winds increases in the spring and autumn seasons in Baghdad [52].

In Baghdad, dust storms are associated with depressions that form over the Red Sea, White Sea and Indian Ocean. These depressions move the air in a motile way toward the center and move in the form of large masses of air, traversing large areas of dry flat lands from west to east. This movement raises and carries dust, decomposing and disintegrating

organic matter and industrial waste. The western plateau of Baghdad is a major source of dust storms that surround this city. Dust storms are frequent, increasing in frequency during the hot season and decreasing in frequency during the cold season. Typically, these storms begin to form in the early morning and peak around midday; they then tend to decrease after 9 PM until 6 AM the next morning [9].

The dust storms that afflict Baghdad province mainly occur during two peak seasons: The end of the spring season and the beginning of the autumn season. Currently, dust storms are also active during the summer due to the northwest winds that are active at noon. These winds that blow on Baghdad pass with a limit of 33.6% of the total winds that pass through the province through the western plateau. These storms cross dry soil and are considered a major funder of the dust of these winds, although they are loaded with dirt and dust from the Levantine desert [53,54]. The reason for the dominance of the northwestern winds over Baghdad can be attributed to the Azorean high, which causes instability in the summer weather of the province due to its proximity to a temperature depression. These pressure systems are the main cause of instability, drought and high air temperature during the Baghdad summer. The Azores high and Indian monsoon low (supported by the subtropical high in the upper atmosphere) contribute to the control of dry air mass at the surface. The dominance of the northwest winds may also be due to the concentration of the indigenous seasonal low east and south of Iraq coinciding with the high atmospheric pressure over the sea causing a pressure gradient, which enables the northwestern winds to prevail over Baghdad Province [55].

Baghdad province is surrounded by a group of mountains and plateaus at not far distances. These plateaus and mountains are home to what is called the plateau breeze, whereby the hotter air in the plateaus rises to replace the thicker and cooler air of the plains. The movement of air from the plateau to the plain carries with it dust particles. The plateau of Badia Al-Sham is characterized by dryness, low vegetation covers and loose soil. It is also characterized by the light weight and ease of transportation of its soil particles. These conditions are favorable for activating dust storms that blow over Baghdad. The city of Baghdad can be considered part of the dust-exporting region as it is surrounded by lands that are capable of exporting dust particles, silt, and loose and fragile clay particles.

In early April 2022, a dust storm covered large parts of Iraq for three days. During this storm, the sky turned an orange color, the visual range decreased and air quality deteriorated. The storm's development between days 7 and 9 of April is shown in Figure 2. These images were taken using the "Visible Infrared Imaging Radiometer" (VIIRS) array on the "NOAA-NASA Suomi NPP satellite" and the "Moderate Resolution Imaging Spectroradiometer" (MODIS) on "NASA's Terra" satellite. The captured pictures show that the dust storm began over northern Iraq on the 7th April, but two days later, it passed Baghdad and extended to southern Iraq. This type of dust storm became common in the summer in Baghdad due to the intense winds that blow from the northwest, called Shamal winds in Iraq. However, this type of wind also occurs in other seasons. In the spring, these winds abound in western Iraq, turning into dust storms and extending to Baghdad most of the time. During the storm of April 2022, dozens of citizens were hospitalized due to respiratory problems. Pictures show that the dust darkened the snow on the mountains in Turkey.

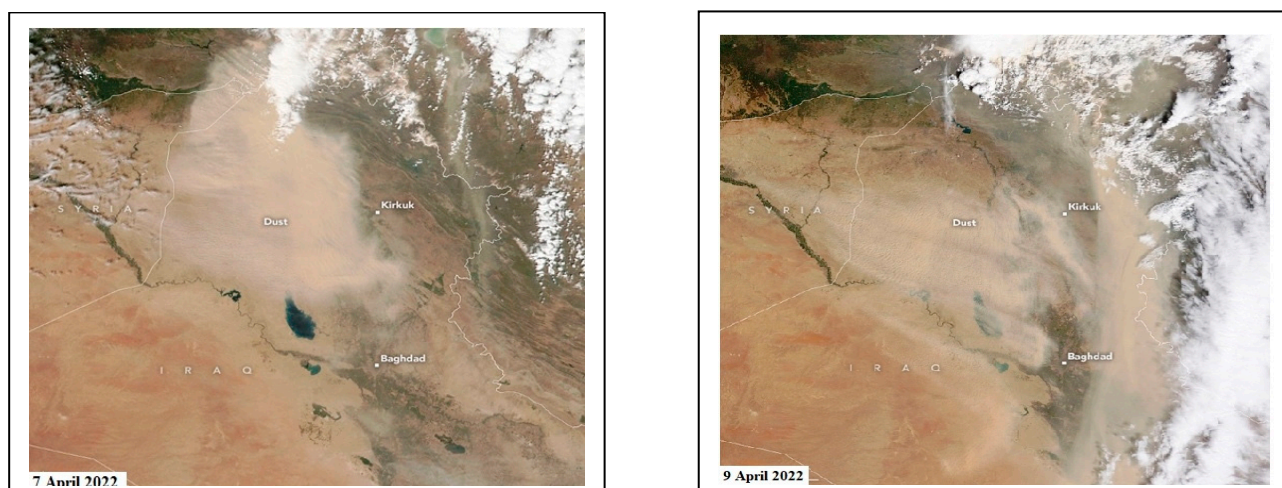


Figure 2. NASA images of the dust storm that crossed Iraq, passing through Baghdad, at the beginning of April 2022.

4. Effect of Dust on Photovoltaic Modules

In the past two decades of the 21st century, the use of PV modules has motivated the production of clean and sustainable electricity. PV technology has broad prospects, especially considering the development of its technologies and low costs [56–59]. The efficiency of PV modules is critically affected by solar radiation intensity and temperature and by shadow and dust [60,61]. The dust particles suspended in the air reduce the amount of radiation falling on the surfaces of the PV modules and their deposition and accumulation on these modules prevent light transmittance. This dust accumulation results in a clear deterioration in the efficiency of power generation [62,63]. Several studies have shown that the electrical efficiency of PV modules decreases by 30% in areas with high dust pollution [64]. The accumulation of solid dust particles on the PV modules completely blocks sunlight in the polluted areas. These contaminated PVs cannot produce electricity and local hotspots are formed on the modules as the ambient temperature increases. This type of dust accumulation of solid and adherent contaminants causes a significant reduction in the productivity of PV modules and, in some circumstances, causes damage [65,66]. The accumulation of a small amount of fine dust on PV modules causes shading that weakens the solar radiation intensity reaching the PV modules [67].

Alnasser et al. (2020) stated that the word “dust” refers to organic and inorganic materials that are suspended in the air and transmitted by their movement over long distances [68]. Dust includes soil particles, smoke, haze, particulate matter, bacteria, pollen grains, etc. Due to the various sources of dust, there are significant differences in size, shape, distribution and concentration. PV modules become contaminated with dust when airborne dust particles settle on the surface of PV modules. Dust build-up on these modules causes a significant decrease in power output [69]. It was estimated by Ilse et al. (2019) that the revenues of PV energy globally decrease by more than USD 5 billion annually due to the pollution of PV modules from dust [70].

The effect of dust pollution on solar energy generation has been intensively investigated in the literature. The increasing effects of climate change and the increase in dust storms around the world coincide with the increasing trend toward installing and operating PV plants, which are often installed in desert locations [71,72]. Empirical studies have been conducted to directly estimate the effect of dust pollution on PV systems. Few of these studies were conducted in the airspace of Iraq and rarely were studies of this kind conducted in Baghdad. Table 1 shows some of these studies on the effect of dust on PV modules in several regions of the world, including Iraq and the city of Baghdad.

Table 1. Studies on the effect of dust accumulation on PV modules in different regions.

Ref.	Location	Year	PV Type	Without Cleaning Exposure Period	Power Loss (%)
Zaihidee et al. [73]	Malaysia	2018	Monocrystalline	1 month	15–45
Alnaser et al. [74]	Bahrain	2018	Polycrystalline	15 months	10
Sidiki et al. [75]	Mali	2018	Monocrystalline	1 month	7
Willoughby and Osinowo [76]	Nigeria	2018	Monocrystalline	Harmattan season	18
Hadwan and Alkholidi [77]	Yemen	2018	Monocrystalline	5 days	16.76
Gholami et al. [78]	Iran	2018	Monocrystalline	70 days	21.47
Hammoud et al. [79]	Lebanon	2019	Monocrystalline	1 year	20–40
Kazem and Chaichan [80]	Oman	2019	Monocrystalline	1 month	5.5–18
Al-Kouz et al. [81]	Jordan	2019	Polycrystalline	50 days	14.3–20
Gupta et al. [82]	India	2019	-	30 days	4–20
Alquthami and Menoufi [83]	Egypt	2019	-	2 weeks	15
Al-Housani et al. [84]	Qatar	2019	cadmium-telluride CdTe	1 month	14
Quansah and Adaramola [85]	Gana	2019	Polycrystalline Monocrystalline HIT silicon, a-Si, CIS	14 months	8–14.8
Alawasa et al. [86]	Oman	2019	Polycrystalline	98 days	45.6
Salimi et al. [87]	Iran	2019	Monocrystalline	45 days	8–12
Lu et al. [88]	China	2020	Monocrystalline	60 min	26–50
Al-Badra et al. [89]	Egypt	2020	Monocrystalline	6 weeks	32.84
Ullah et al. [90]	Pakistan	2020	Polycrystalline	25 days	22.5
Kazem et al. [91]	Oman	2020	Polycrystalline	1 year	6.3
Majeed et al. [92]	Pakistan	2020	Monocrystalline Polycrystalline	1 month	16.16 11.54
Semaoui et al. [93]	Algeria	2020	Monocrystalline	1 month	8.79
Mustafa et al. [94]	Jordan	2020	Polycrystalline	21 days	8.8
Darwish et al. [95]	United Arab Emirates	2021	Monocrystalline	2 months	30
Al Bakri et al. [96]	Jordan	2021	Monocrystalline	1 day	2.3
Yazdan and Yaghoubi [97]	Iran	2021	Monocrystalline	Summer season	6.9–7.7
Kenedy et al. [98]	United Arab Emirates	2021	Polycrystalline	2 weeks	14%
Lasfar et al. [99]	Mauritania	2021	Polycrystalline	3 months	21.57
Hamid et al. [100]	Egypt	2021	Polycrystalline	75 days	53
Zeedan et al. [101]	Qatar	2021	Polycrystalline	6 months	43
Kazem et al. [102]	Oman	2022	Monocrystalline Polycrystalline	35 days	14–31 17.14–28.1
Sevik and Aktas [103]	Turkey	2022	Polycrystalline	1 month	4
Yazdani and Yaghoubi [104]	Iran	2022	Monocrystalline	1 day	1.7–4.4
Enaganti et al. [105]	India	2022	Monocrystalline Polycrystalline	120 days	7.94–17.48
Juaidi et al. [106]	Palestine	2022	Monocrystalline	7 months	9.99
Abdulazeez [107]	Iraq	2018	IRAQ Monocrystalline	1 month	30.4
Hameed et al. [108]	Iraq	2019	Polycrystalline	7 days	4.12
Jasim et al. [109]	Iraq	2021	Polycrystalline	15 days	5.93
Abbas et al. [110]	Iraq	2021	Monocrystalline	3 months	72.4
Chaichan and Kazem [111]	Iraq	2020	Baghdad APM-P Monocrystalline	7 days	27 24.6
Mahmood et al. [112]	Iraq	2020	Polycrystalline Cadmium Telluride Thin film	1 year	24.4 25.14 26.6
Kazem et al. [113]	Iraq	2021	Monocrystalline	7 days	4.2

Table 1 confirms that the accumulation of dust on PV modules (irrespective of their type, installation location or angle of inclination) deteriorates their electrical productivity. To protect PV modules from this deterioration, periodic cleaning must be conducted at specific intervals. However, none of the studies in Table 1 addressed how the accumulated dust can be tolerated by PV modules, how to deal with the modules, or the recommended quality and timing of cleaning during emergency incidents. The study area (Baghdad, the capital) has immense potential for solar energy as it has high irradiation, which makes it perfectly suitable for operating PV energy systems to achieve sufficiency in electricity [114]. Solar energy in Baghdad as a source of renewable energy has greater potential than wind energy. Unfortunately, this energy is not fully exploited, but, currently, there are opportunities for the Baghdadi citizen, represented in soft loans, while reducing costs and installing and operating PV systems. Currently, the Iraqi government is planning to build seven stations in different regions of the country with a capacity of 750 MW as a programmed transition toward environmentally friendly government policies [115]. Iraq is an oil country and one of the richest countries in the world in terms of natural gas and oil reserves; these conditions represent an internal weakness because the country depends on fossil fuels to generate electricity due to their availability and cheapness. Additionally, the climatic risks of dust and dust storms that reduce the productivity of PV modules, in addition to the political instability in the country and the change in the decision to use alternative power, pose risks to the development of the infrastructure of high-power PV stations.

This situation thus triggers the idea of the current study as Baghdad was subjected to two major storms during the month of March 2022. The necessary equipment has been prepared to study the effect of dust winds and dust storms before and during storms in Baghdad and three days after their demise. A severe dust storm occurred from the 7th to the 9th of April, when the measurements were taken. There have been similar studies conducted in Iran and Saudi Arabia using satellite images and NASA, but they did not document experimentally the deterioration of PV modules, as in the current study. In this study, experimental measurements were made of the effects of the dust storm that lasted for three days from 7th April to 9th April 2022 on PV modules in Baghdad. This study assesses the impact of such storms and presents proposals based on a practical study that can affect decision-makers who are vacillating between adopting sustainable solar energy or remaining on fossil fuels as a primary source of electric power generation.

5. Experimental Setup

5.1. Study Area

Baghdad is the capital of Iraq and the center of the Baghdad Governorate. This city is considered the largest city in Iraq in terms of its population, which exceeded 8.5 million citizens in 2016 [115]. The city is the economic, administrative and educational center in the country. This city has an old historical status as it was the capital of the Abbasid Caliphate and the most important center of science and culture for centuries. Baghdad's geographical location is characterized by abundant water and an insignificant risk of flooding. Baghdad is located at longitude forty-four and latitude thirty-three and the Tigris River bisects it into two halves. Baghdad mediates the northern and southern cities of Iraq. Figure 3 shows an aerial view of Baghdad, through which the Tigris River passes.



Figure 3. An aerial view of Baghdad city divided by the Tigris River.

Baghdad is characterized by a desert climate and there have been hot summers plagued by dust storms in the area in recent years. Experts referred to the intensification and recurrence of these storms in the summer in Baghdad after the war in 2003 and to the change in the Iraqi environment as a whole as a result of deliberate neglect and failure to develop urgent solutions, in addition to global warming resulting from the high carbon content in the atmosphere, which was caused by many facilities, such as the Dora refinery and energy production plants using fossil fuels (South Baghdad station, Dora station and North Baghdad station). Exhausts from electric generators, which number more than thousands, also play a crucial role in increasing carbon pollutants in the city's atmosphere. Desertification has increased in the areas surrounding Baghdad and soil erosion due to more than four continuous decades of drought [115]. Table 2 shows the weather conditions for the city of Baghdad for the year 2020.

Table 2. Average climatic conditions for Baghdad City for the year 2020.

Condition	Jan	Feb	March	April	May	June	July	August	Sep	Oct	Nov	Dec	The Average
Irradiation period (h/day)	6.1	7.2	7.9	8.6	10	11.4	11.3	11.1	10.1	8.2	7.1	6.1	8.7
Irradiance intensity (W/m^2)	287	362	485	536	657	728	792	846	733	682	511	420	587
Maximum air temperature ($^{\circ}C$)	15.8	18.7	23.8	30.2	36.8	45.8	47.3	50.8	42.2	35.6	23.7	17.6	32.4
Minimum air temperature ($^{\circ}C$)	4.2	5.9	10	15.6	20.6	23.8	25.9	25.3	21.2	16.5	9.8	5.6	15.4
Wind velocity (m/s)	2.6	2.9	3.2	3.2	3.3	3.8	4	3.5	2.8	2.6	2.5	2.4	3.1
Relative humidity (%)	71.2	57.3	50.4	43.6	31.7	25.1	24.7	26.7	31.8	42.1	57.8	69.3	44.3

5.2. Instrumentations

Concentrations of ultrafine airborne dust particles (PM1.0, PM2.5 and PM10) and total suspended dust particles (more than PM10) were measured using the “Met One Model GT-521”. This device works with a laser photometer and was carefully calibrated at the “Central Organization for Standardization and Quality Control” in Baghdad just before the experiments were conducted. The device was installed at heights of one, two and three meters above the surface to ensure multiple readings for measuring dust particle concentrations. The readings were conducted every 10 min for each height and repeated three times each to confirm repeatability. The device readings uncertainty was 0.3%. The measurements procedure started with the Meteorological Authority warning of a dust

storm that started to form in northwestern Iraq on 6th April in the evening and lasted after the storm for three days (12th April).

Several measuring devices were used in the current study. A sensitive scale (EJ6I0-E) with an accuracy of $\pm 0.36\%$ was used to weigh the amounts of accumulated dust. To control the load achieved on the PV modules and their current and voltage values, an “Eisco Rheostats type resistance” (1325 ohms, dimensions $130 \times 25 \times 40$ mm with a maximum current of 0.5 A) was adopted. A digital voltmeter (200 mV: 500 V DC or 350 V AC RMS) with an accuracy of $\pm 0.5\%$ and a digital ammeter with an uncertainty of $\pm 1.0\%$ was used in the measurements. A mercury scale was used in the shade to measure ambient air temperatures before, during and after the storm. The accuracy of this scale was $\pm 0.5\%$. Measurement of the intensity of the light shining on the PV modules in the experiments were presented using an intensity meter type (MT-4617); its accuracy was $\pm 0.3\%$. To measure the solar radiation intensity, a solar radiation intensity meter type MP-200 was used. This device has an uncertainty of $\pm 0.44\%$.

5.3. Photovoltaic Modules

As it is difficult to estimate a specific period or day for the occurrence of a dust storm, 12 PV modules were prepared and their specifications are shown in Table 3 and Figure 4. Dust density losses were calculated for identical PVs by comparing dusty and clean PVs under the same conditions. The daily electricity generation losses were the sum of density losses for a day. Dust density measurements were taken for the PV modules, starting from 1st April 2022, daily for one of the PV modules, every two days for the second module, every three days for the third module and so on to determine the dust density, losses and electricity generation losses for daily and multi-day accumulation. Dust density was measured by the weight of the PV module at dawn before the start of the measurements (completely clean) and after sunset (dusty). The dust storm began on the 7th of April; thus, module no. 7 (which became no. 1 in the sequence) was considered to be the dust that accumulated on the first day of the storm. PV module no. 8 (which became no. 2 in the sequence) represented the accumulation of dust after two days, while module no. 9 (which became no. 3 in the sequence) represented the accumulation of dust after three days of the dust storm. Module nos. 10, 11 and 12 represented the accumulation of dust after the storm. These measurements after the storm were particularly important as the wind speed began to calm down after the storm had passed and the fine dust particles suspended in the air began to precipitate. Lightweight PV modules were used to facilitate the transportation of dusty modules from the outdoors to the laboratory easily while reducing accumulated dust vibration in a way that causes disturbance to the particles settled on the surface. PV modules were installed on the surface of the ground horizontally in order to receive the highest possible amount of sedimented dust.

Table 3. The used PV panel specifications.

Panel Type	Polycrystalline
Maximum power (Pm)	10 W
Maximum power voltage (V _{pm})	17.3 V
Maximum power current (I _{pm})	0.59 A
Current (short circuit)	0.64 A
Voltage (open circuit)	21.8 V
Module efficiency	9.5%
Weight	1.4 kg
Module's area	358 mm × 310 mm



Figure 4. PV modules assortment and their arrangement.

5.4. Solar Simulator

In this study, a solar energy simulation system was used inside the “solar energy laboratory at the Energy and Renewable Energies Technology Center at the University of Technology”. Figure 5 shows 23 “Halogen Brillanta lamps” that were used in the solar simulator which produce solar irradiance of 0–1000 W/m². The simulator consisted of nine columns with two or three lamps per column. The total area of the solar simulator was 1.40–1.22 m, with a 30 cm distance from the PV module. One of the advantages of this system was the ability to control the intensity of lighting. Figure 5 illustrates the solar simulation system used in the tests. By adjusting the distance between the lights, the intensity of the light could be controlled and distributed evenly on the surface of the PV board.



Figure 5. Solar simulator used in tests.

The PV module’s power is calculated by

$$P = I_{mp} \times V_{mp}$$

The electrical efficiency of the PV module is

$$\eta_{el} = \frac{P_{mp}}{I_s \times A_{panel}}$$

The loss ratio due to soiling is calculated using the following equation:

$$\% \text{ Power loss} = \frac{P_{clean} - P_{dusty}}{P_{clean}}$$

The drop in module’s electrical efficiency:

$$\% \eta_{drop} = \frac{\eta_{clean} - \eta_{dusty}}{\eta_{clean}}$$

After the indoor experiments for each PV module, the accumulated dust was collected using a brush and weighed on a sensitive scale. Figure 6 shows the amounts of dust accumulated on the modules for each day of the measurements. It seems that during the two days before the storm, the airspeed increased and caused an increase in airborne dust that accumulated on the PV modules. During the storm, the accumulated dust was at prominent levels compared to the previous days. After the storm, the level of accumulated dust remained high compared to the days preceding the storm, although it was lower than the days of the storm.

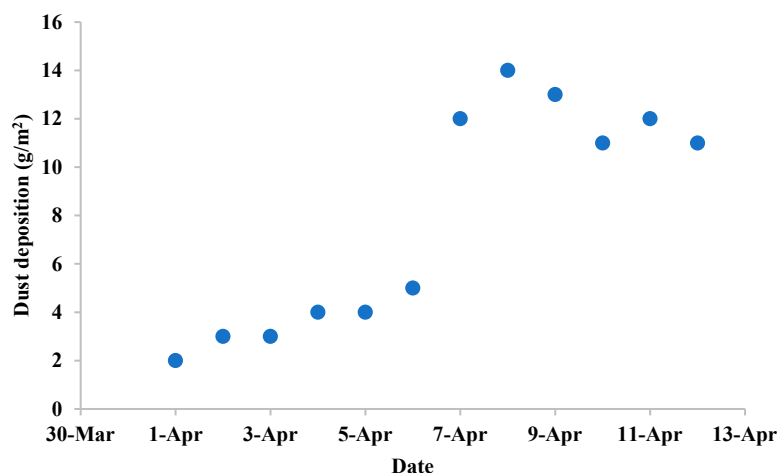


Figure 6. Daily dust deposited on PV modules throughout the test days.

5.5. Uncertainty Analysis

The measuring devices used in this study were calibrated and the accuracy of the devices was determined by determining the value of the empirical error. The uncertainty equation adopted was proposed by Holman (2012) [116]:

$$e_R = \left[\left(\frac{\partial R}{\partial V_1} e_1 \right)^2 + \left(\frac{\partial R}{\partial V_2} e_2 \right)^2 + \dots + \left(\frac{\partial R}{\partial V_n} e_n \right)^2 \right]^{0.5}$$

where e_R represents the total uncertainty in the results, R indicates a function of the independent variables (V_1, V_2, \dots, V_n) or ($R = R(V_1, V_2, \dots, V_n)$), e_i symbolizes the uncertainty interval in the n th variable and $\frac{\partial R}{\partial V_1}$ is the measured result sensitivity for a single variable.

Table 4 lists the instruments used in the tests and their uncertainty. In this study, the uncertainty was found for each of the dust-measuring devices and the electrical variables measuring devices separately to ensure that no examination was affected by other tests; then, the total uncertainty was calculated.

Table 4. The instruments’ uncertainty.

Instrument	Parameter	Uncertainty Value
Met One Model GT-521	ultrafine and coarse dust particles concentrations	±0.3%
EJ610-E	sensitive scale	±0.36%
Digital voltmeter	voltage	±0.5%
Digital ammeter	Current	±1.0%
Thermometer (Mercury)	Ambient temperature	±0.5%
Intensity meter (MT-4617)	Lights intensity	±0.3%
Intensity meter (MP-200)	Solar intensity	±0.44%

Ultra-fine, fine and coarse particle concentration uncertainty:

$$\sqrt{(0.3)^2 + (0.36)^2} = \mp 0.468\%$$

Electrical parameters uncertainty:

$$\sqrt{(0.5)^2 + (1)^2 + (0.5)^2 + (0.3)^2 + (0.44)^2} = \pm 1.335\%$$

Overall test uncertainty:

$$\sqrt{(0.468)^2 + (1.335)^2} = \pm 1.414\%$$

The uncertainty values for measurements of dust concentrations and electrical parameters were less than 5%; therefore, the obtained measurements were considered geometrically acceptable and reliable.

5.6. Test Procedure

After several moderate-intensity dust storms hit Baghdad in March 2022, meteorologists warned of severe storms of this kind in the coming days. Preparations were made for the severe storm study by laying 12 PV modules on the roof of the “Energy and Renewable Energies Technology Center at the University of Technology—Baghdad”. The dust accumulated on it was measured and its performance was checked, as detailed in the PV module section. On the first day, the power output of the module was measured from 8 AM until 5 PM. After that, the module was lifted very carefully and installed in the solar simulator and its energy output was checked at a variable solar radiation intensity (from 8 to 9:30 AM the subjected irradiance was 200 W/m², from 9:30 AM to 3:30 PM the subjected irradiance was 300 W/m² and from 3:30 to 6 PM the subjected irradiance was 200 W/m² again, adopting the procedure by Al-Waeli et al. (2018) [117]. This radiation intensity was chosen from practical measurements taken during previous storms and was the lowest radiation intensity measured at that time. Additionally, the indoor air temperature of the laboratory was kept constant at 25 °C. This temperature was chosen because it represents the standard measuring temperature. The PV module was cleaned and placed in a new arrangement so that its number was 13 and so on. To ensure the complete cleanliness of the PV modules used, they were cleaned with a sodium solution to eliminate any sulfur or carbon particulates that may have been precipitated with dust, depending on the results of Chaichan et al. (2015) [8]. The idea of this method is to measure the effect of dust accumulation on PV modules during storm strikes as soon as they occur. Inside the laboratory, the effect of dust accumulation on the PV module was measured only without the presence of dust suspended in the air. The difference between the two values indicates the effect of suspended dust and the severity of its effect on the module’s productivity. During the analysis of the experimental measurements and because the fluctuation in the measured parameters was large, the average solar radiation, air temperature and power output measurements of the modules for the three days before the storm were taken as the pre-storm average. The arithmetic average of the measured readings was calculated during and after the storm. The reason for this was to demonstrate the effects on PV modules to ensure their correct disposal.

6. Results and Discussions

Figure 7 shows the average intensity of solar radiation measured for the city of Baghdad before, during and after the storm. The solar radiation intensity before the storm was high, reaching values of approximately 720 W/m². The intensity of the solar radiation deteriorated sharply during the storm and decreased by 50.54%. The intensity of the solar radiation outside the storm in the atmosphere did not change, but its intensity inside the storm dissipated, spread and was reflected by dust and sand loaded in the air. After the

storm, large dust particles were deposited and fine and ultra-fine dust particles remained suspended in the air. These particles reduced the intensity of solar radiation after the storm compared to measurements taken before the storm. When comparing measurements, it was found that the deterioration in radiation intensity reached 13.87%.

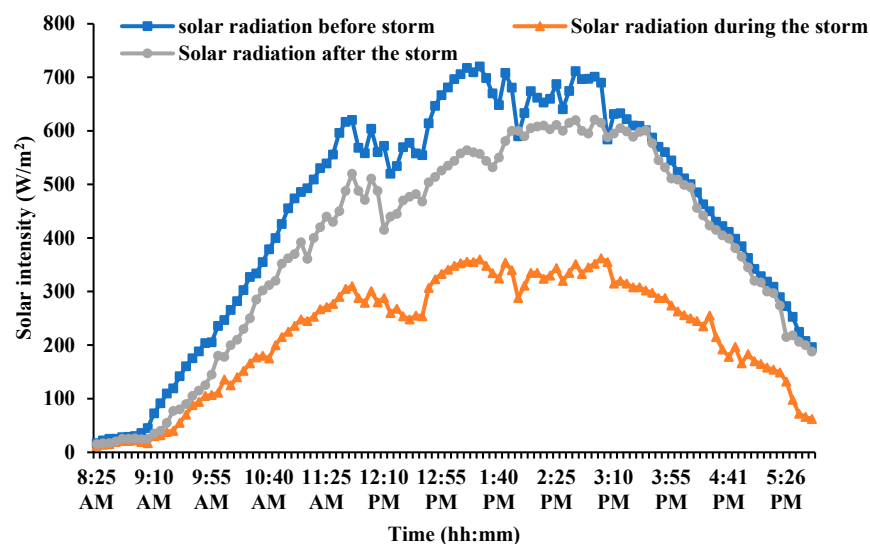


Figure 7. Solar radiation intensity before, during and after the dust storm.

Figure 8 shows the impact of the dust storm before, during and after the storm on ambient temperatures. The ambient temperature decreased due to the impact of the dust storm, which reduced the direct solar radiation intensity and dispersed a large part of it. Additionally, the mass of dust suspended in the air absorbed a large part of this radiation intensity, which reduces the air temperature. The average decrease in the temperature reached 21.09% during the storm compared to the previous days, which was a high percentage. After the storm, the suspended mass of dust was still clear as the large particles had been deposited, but the fine and exceptionally fine particles remained suspended for days and sometimes months, as indicated by Kazem et al. (2014) [9]. By comparing the temperatures after the storm with those from the days before the storm, a decrease of approximately 12.68% was observed. The greatest effect of the PV panel's temperature was on the generated current as it decreased with this temperature increase, as shown by Al-Waeli et al. (2017) [118]. The results of Figure 8 show that the temperature rise of the PV panel during and after the storm was not significant; thus, the effect of the panel temperature on the current and voltage measurements was limited during this period.

In Figure 9, particulate matters were measured instantaneously using the "Met One Model GT-521". Figure 9 shows the concentration of PM1.0, which is considered the most dangerous particulate matter to human and animal health. Particles of this size can reach the most accurate alveoli and capillaries of the lung and concentrate in them, causing their obstruction, and their damage may develop into serious lung diseases. Hamza et al. (2020) showed that the extent to which these particles are dangerous depends on their chemical composition [119]. Since Baghdadi dust is loaded, in addition to particles of silicon oxide, with particles of a carbon source produced from the Doura refinery and the three power stations, in addition to thousands of private generators, the health risks involved increase sharply. The results of the operation show a clear increase in PM1.0 during the storm up to 569.9% compared to levels before the storm. After the air speed decreased and the large particles began to precipitate, these particles withdrew a large part of the PM1.0 adhering or close to them and deposited them on the surface of the PV modules. However, the measurements show that the levels of PM1.0 after the storm were also high and reached 69.7%.

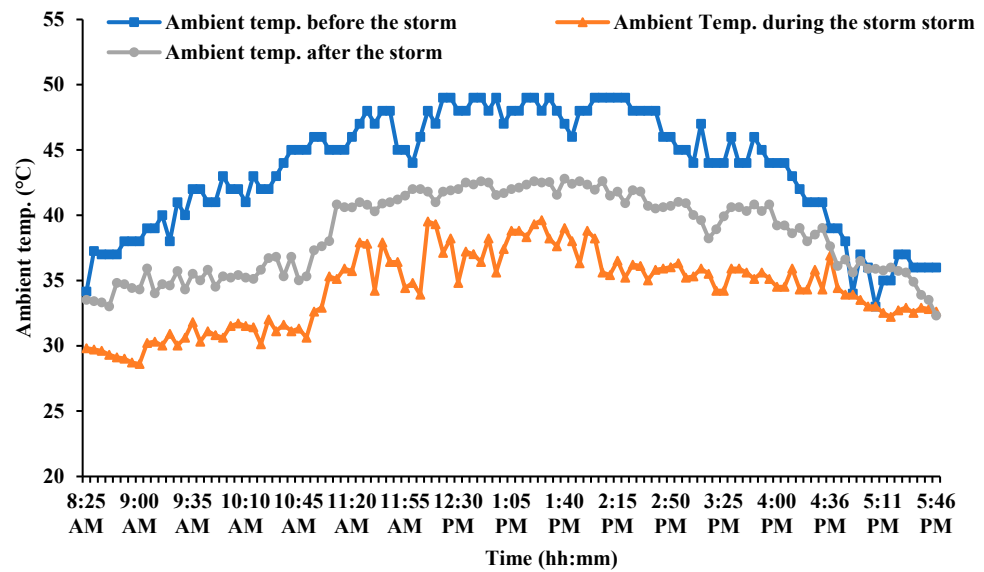


Figure 8. Ambient temperature before, during and after the dust storm.

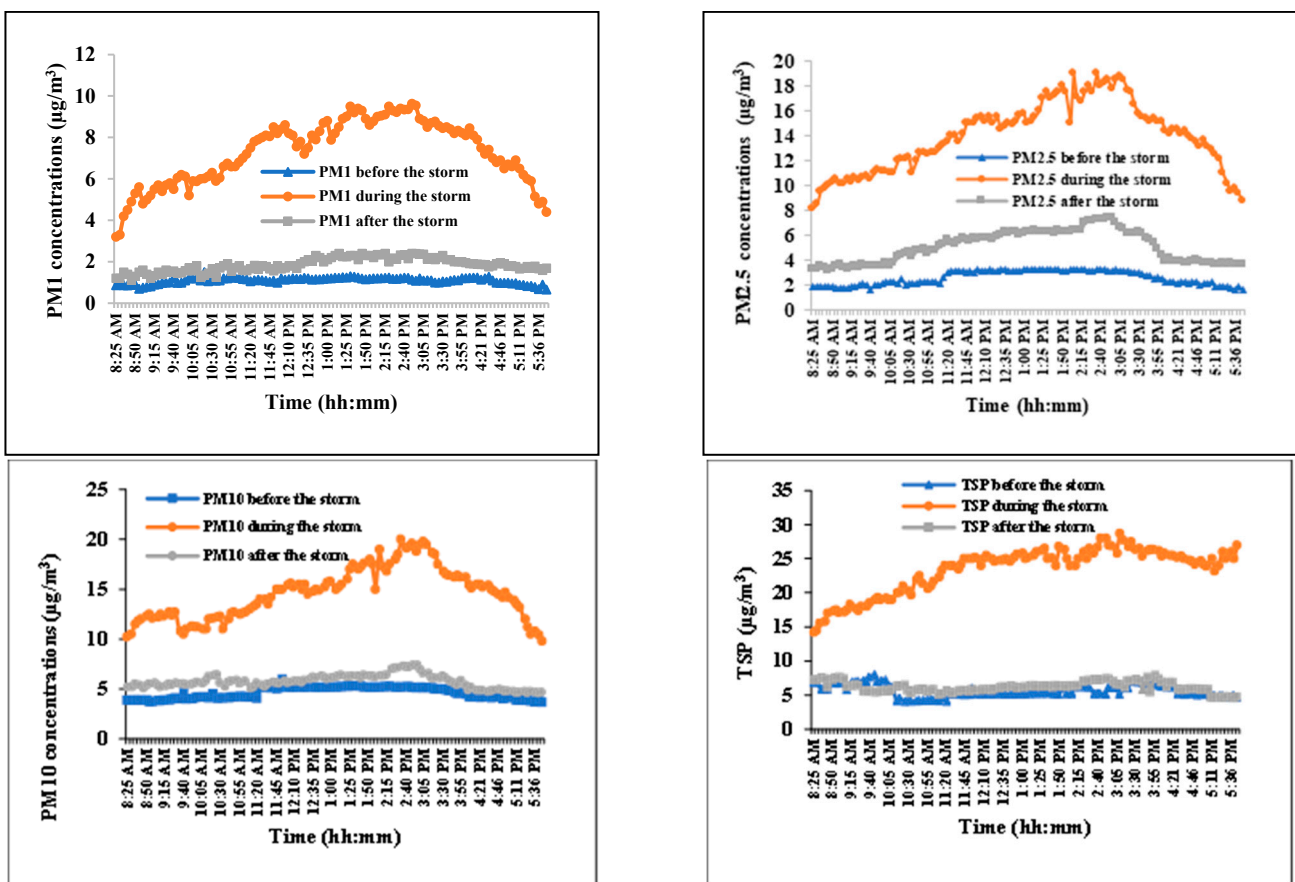


Figure 9. Ultra-fine, fine and coarse particle levels before, during and after the storm event.

Figure 9 shows practical measurements of PM2.5, which is no less dangerous. These ultra-fine particles enter the respiratory tract and bloodstream and interact with them, causing several health risks, depending on their components. The concentration of PM2.5 increased by 441% during the storm compared to pre-storm levels. When the storm passed through Baghdad, it carried with it a large part of the PM2.5 attached to it, causing its levels to drop, in addition to the precipitation of part of it after the air velocity calmed down.

PM_{2.5} concentrations after the storm were approximately 36.34% higher than their levels before the storm.

Figure 9 shows the concentrations of PM₁₀ in the air before, during and after the storm. PM₁₀ levels increased during the storm by 217.22% compared to levels before the storm. After the calm of the storm, PM₁₀ concentrations were higher than their levels before the storm by 25.05%. This result shows that larger particles were deposited faster, while finer particles remained suspended in the atmosphere.

Total suspended particles (TSP) are particles with a diameter of more than 10 nanometers. These particles, in addition to being deposited on the surface of PV modules, are dangerous in that they carve into the cell glass and cause scratches and corrosion. Figure 9 shows the concentrations of these particles suspended in the air before, during and after the storm. The TSP concentrations increased during the storm days by 319.21% compared to the previous days and were responsible for the scattering of sunlight and the absorption of part of the air heat. These particles precipitated quickly after the storm subsided due to their weight, and their concentrations decreased by 309.1% compared to the storm days, but they remained higher than their levels before the storm by 10.11%. The high risks of these particles during the storm were reduced afterward. However, it is particularly important to know the chemical components of these particles to determine the required cleaning methods. For example, it is not recommended to clean calcium carbonate particles, white cement or gypsum with water as they interact with the water to form a cohesive layer that is difficult to be removed from the surface of the PV panel, as indicated by Alnasser et al. (2020) [68]. Additionally, the PM particles accumulated on the PV surface accumulated (the bulk of which are carbon and sulfur molecules) are not recommended to be cleaned with water because water is not effective in removing them. It is preferable to use a sodium solution, as indicated by Chaichan et al. (2020) [111].

In the set of experiments conducted inside the laboratory, the performance of the PV modules was measured at a constant radiation intensity (300 W/m^2) and constant indoor temperature ($25 \text{ }^\circ\text{C}$), as shown in Figure 10. Current and voltage measurements began at sunrise and ended at sunset. Indoor measurements were conducted with solar radiation intensity and air temperature set at 300 W/m^2 and $25 \text{ }^\circ\text{C}$, respectively. In Figure 10, the effect of dust accumulated on a PV module during a dust storm on the current is shown. As has been proven in most previous studies, the clearest effect of accumulated dust is on the current generated by the PV module. The dust accumulated during the dust storm caused a deterioration of the current generated by the PV module by an average of 32.28% of the pre-storm value. Additionally, after the storm had passed, the current generated was not fully restored but remained at a lower rate of approximately 12.43%.

The effect of the dust storm on the voltage of the PV module was less effective than the state of the current, as shown in Figure 10. The dust build-up caused by the dust storm caused a voltage drop of 14.45% compared to the days before the storm. Part of these losses was recovered after the storm because the accumulated dust was large; thus, the voltage losses for the days after the storm were 8.6% compared to the days before the storm.

The deterioration of the current and the clear decrease in voltage due to the accumulation of dust during the storm caused the collapse of the power generated by the PV module, as shown in Figure 10. The deterioration in the produced power during the storm reached 38.52% as a result of the accumulation of dust. However, after the storm subsided, the generated power did not return to its original state and remained less than the power generated before the storm by 18.66%. Importantly, the dust accumulated on the PV modules and its densities inside the laboratory did not equal that accumulated on the modules outside the laboratory. In the case of outside the laboratory, with the continuous rapid air movement, dust particles, especially those with large diameters, were scavenged.

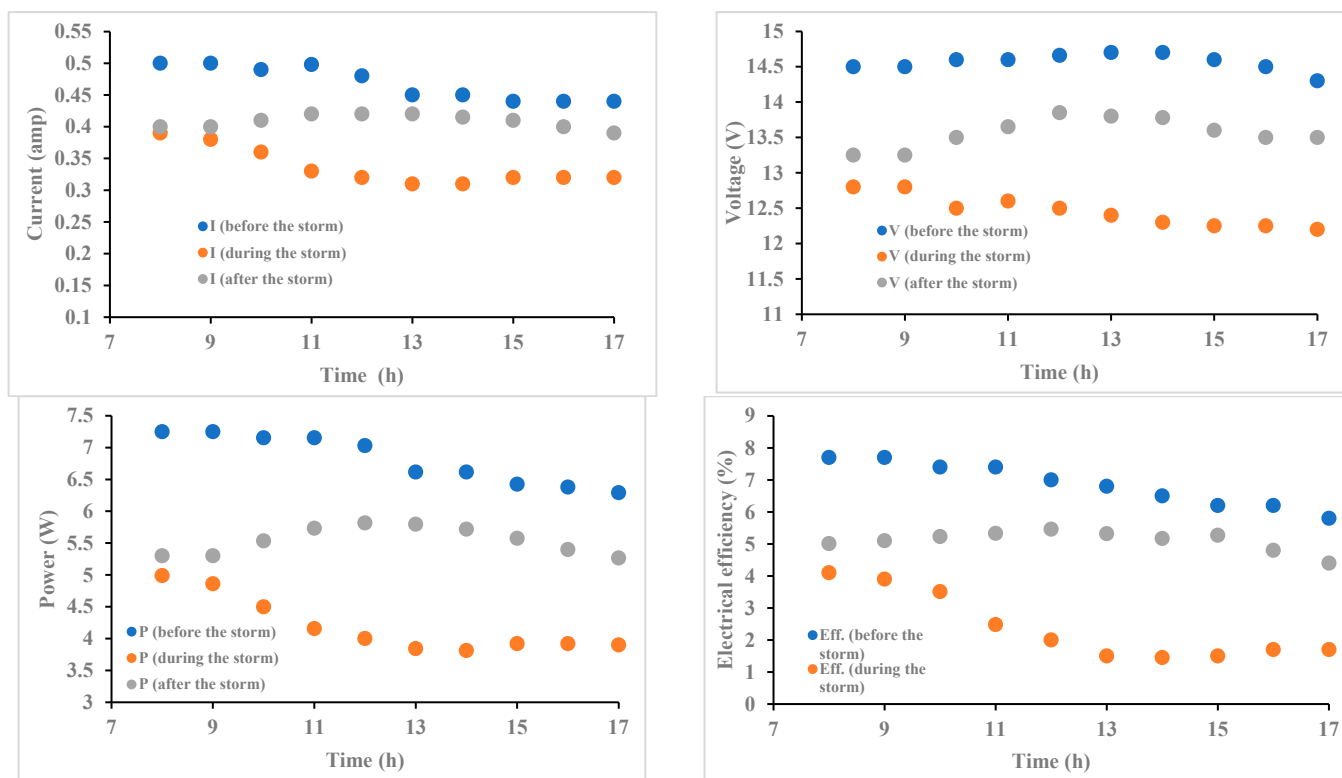


Figure 10. Dust storm impact on PV module performance (indoor tests).

Certainly, the deterioration of the generated power caused a corresponding decrease in the electrical efficiency of the PV module. Figure 10 shows that this efficiency decreased significantly for modules exposed to dust accumulation during the storm, bringing this decrease to 65.58%. As for the days that followed the storm, the efficiency decreased by 25.63% compared to pre-storm conditions. It is notable that the values of electrical power and efficiency at 8 AM were close during and after the storm, while the latter was still less (during the storm). At the beginning of the morning, the effect of radiation intensity was low and the air temperature was appropriate, which reduced their effects on the panels; this is in line with the results of [78,92,99]. The results of Figure 10 clearly show that the dust accumulated during the storm caused significant deterioration that could not be eliminated as cleaning modules during an ongoing dust storm is futile. In the days following the storm and due to the amount of dust suspended in the air, it is preferable to clean with a dry brush (without using any liquid).

Figure 11 presents the outdoor tests of the PV modules before, during and after the storm, which were measured outside the laboratory under real conditions. Here, there were two important effects on the PV modules. The first was the accumulation of dust on the PV modules and the second was the clear decrease in the solar radiation intensity because of its dispersion due to airborne dust. The suspended dust in the air density during and after the storm caused a high deterioration in the solar radiation intensity (as Figure 7 illustrates), followed by a clear decrease in ambient temperatures (Figure 8). Therefore, the influence of temperature during the period of measurements during and after the storm can be ruled out. Figure 11 shows the effect of the studied external conditions on the PV current. The measurements show a significant deterioration in the generated current during the storm as the produced current was 60.24% less than its state before the storm. The deterioration reduced during the days after the storm, bringing the decrease in the generated current to 16.89%. By comparing the results of this figure with those shown in Figure 11, a high deterioration is observed in the case of natural conditions (60.24%) compared to storm conditions (32.28%) (Figure 8). The difference here was caused by a

significant decrease in irradiance during the storm compared to the fixed intensity with which the experiments were conducted in the laboratory. The voltage depended on the solar radiation intensity reaching the PV module; thus, a clear deterioration appeared in the voltage due to the dust storm, as shown in Figure 11. The voltage dropped by 30.7% compared to the generated voltage before the storm. The voltage for the days following the storm decreased by 8.7% compared to the same days. Comparing the results of the indoor and outdoor experiments, significant differences were observed. During the storm, the deterioration was approximately 30.7% externally, but internally, the deterioration was approximately 14.45%. The difference here was caused by the degradation of the direct solar radiation falling on the PV modules as a result of its dispersion, refraction, reflection and absorption by atmospheric dust particles. Similarly, in the days following the storm, the external deterioration (8.7%) was higher than the decrease in the internal experiments (6.8%) for the same reason as the dust suspended in the air during these days was more than for the days before the storm.

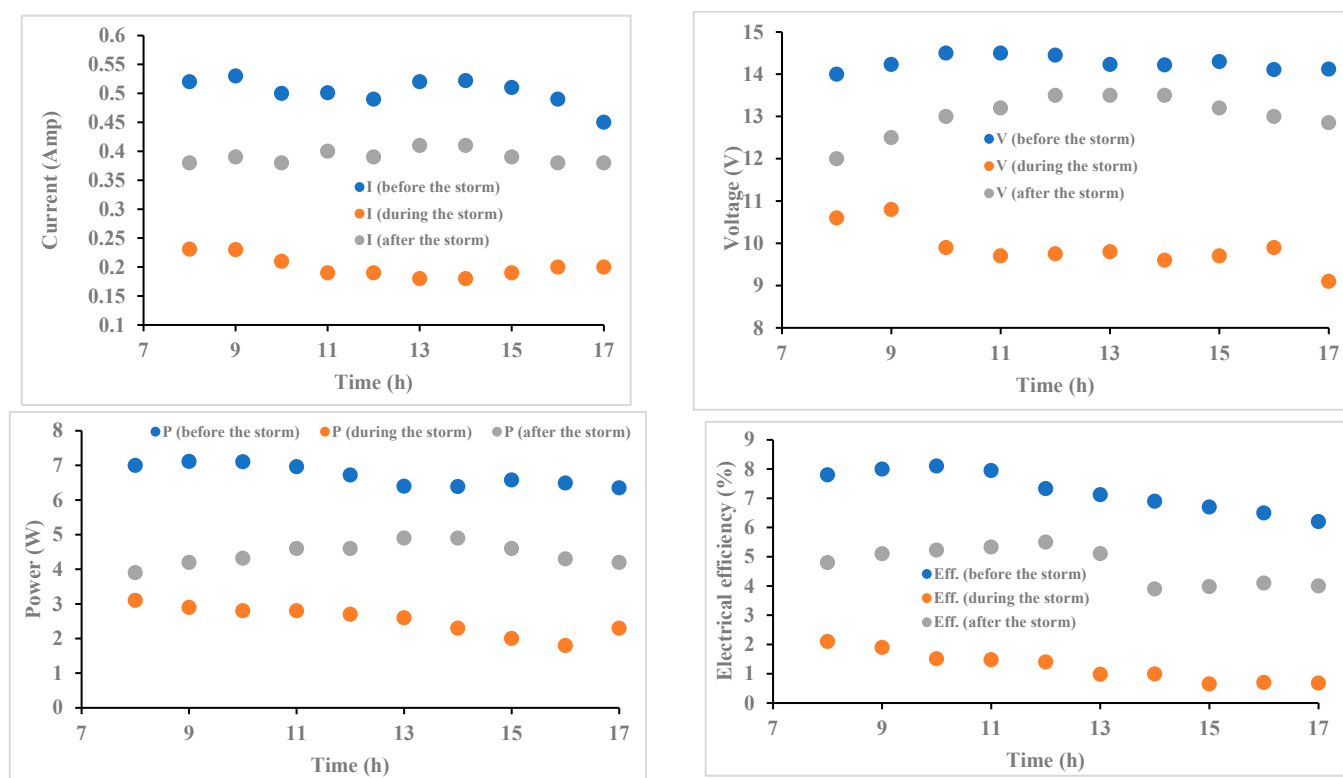


Figure 11. Dust storm impact on PV module performance (an outdoor test).

The current and voltage deterioration was reflected in the generated power, which deteriorated to low levels. Figure 11 shows a decrease in the PV power by approximately 62.3% compared to the days preceding the storm, meaning that the system was not fit to generate the required power, generating in these conditions a third of its designed capacity. Additionally, in the days following the storm, the power decreased by 33.66% compared to the days before the storm. The need for dry cleaning immediately after the storm has passed to reduce the deterioration in the performance of the system must be emphasized here. Figure 11 shows losses in electrical efficiency that reached 82.93% and 19.35% for the days during and after the storm, respectively, compared to the days before the storm. The decrease in the solar radiation intensity and the accumulation of dust on the PV module caused this significant decrease in electrical efficiency.

When comparing the current, voltage, power and efficiency at 8 AM between Figures 10 and 11, it is notable that the difference between the data taken during and after the storm is already visible (Figure 11). The measurements inside the laboratory ex-

cluded two important overlapping effects that existed in the outdoor experiments, namely, the fluctuation in the solar radiation intensity, which was greatly affected by the density of dust in the atmosphere (which was excluded inside the laboratory). Secondly, the deterioration of the radiation intensity caused a clear decrease in the temperature of the PV panels and neutralized this effect. Here, it must be emphasized that the cooling effect of the air movement should be taken into account, the effect of which interfered with the deterioration of the radiation intensity and the decrease in temperatures. Moreover, there was a possible effect of post-storm winds, although the wind speed decreased, but may be responsible for removing some dust particles (especially large ones) so that the electrical parameters slowly returned to pre-storm values. After the storm passed, the density of dust suspended in the air (Figure 9) decreased significantly, increasing the intensity of solar radiation reaching the modules. Despite dust accumulation on the PV panels, this rise in irradiance resulted in an increase in electrical parameters.

Figure 12 shows the average deterioration in the generated power per day during the study period accompanied by the dust accumulation density for the same days. The results show that the power degradation rate was closely related to the severity of the pollution effect because higher surface dust densities correspond to lower power generation. Additionally, the differences in power degradation rates between the outdoor and indoor measurements were very clear. The main reason for this is that in the outdoor measurements, there was no control of the solar radiation intensity, which deteriorated to a large and effective degree compared to using constant solar radiation in the indoor tests.

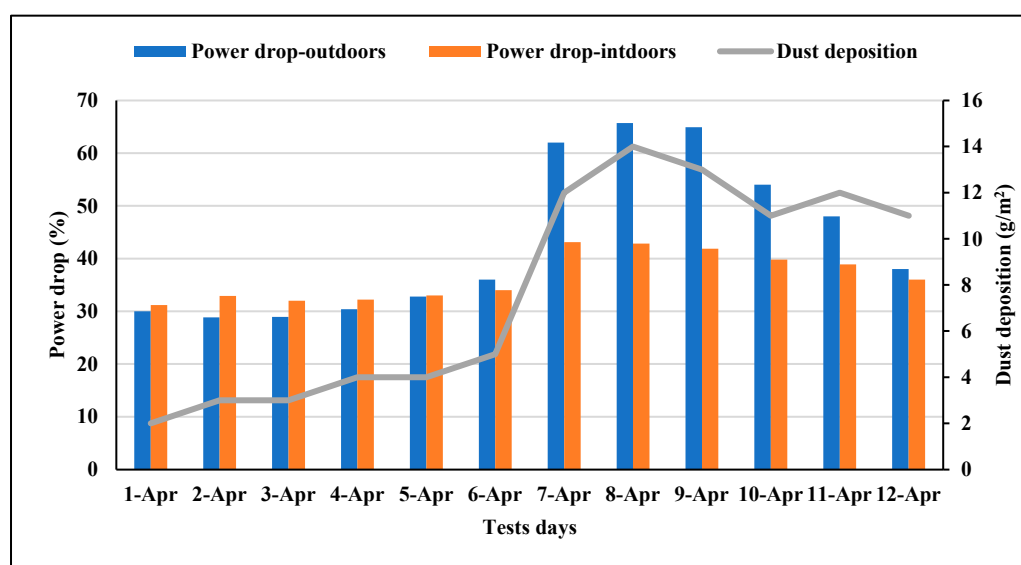


Figure 12. Average daily power drop during the test days.

7. Conclusions

Severe dust storms cause many difficulties and diseases and reduce the effectiveness of photovoltaic modules. In this study, the sources of dust and dust storms that hit Baghdad and their movement were reviewed and investigated. Practical measurements were also taken during the storm that swept Baghdad from the 7th to the 9th of April 2022 that had not been taken before in this city. Practical measurements showed a deterioration in solar radiation intensity by up to 54.5% compared to the days prior to the storm. The ambient air temperature during the storm decreased by 21.09% compared to the days before the storm. Regarding the measurements of ultrafine aerosol particles PM_{1.0} and PM_{2.5}, there was a significant increase of approximately 569.9% and 441%, respectively, compared to the days before the storm. The concentrations of PM₁₀ and TSP increased by 217.22% and 319.21%, respectively. Indoor performance experiments showed a deterioration of current, voltage, power and electrical efficiency by 32.28%, 14.45%, 38.52% and 65.58%, respectively, as a

result of dust accumulated during the days of the storm compared to the days before it. In the outdoor experiments, the rates of deterioration in current, voltage, power and electrical efficiency were greater, reaching 60.24%, 30.7%, 62.3% and 82.3%, respectively, during the storm days compared to the days before it. Additionally, practical measurements showed that the three days following the storm carried high concentrations of PM1.0, PM2.5, PM10 and TSP, reaching 69.7%, 94.67%, 25.5% and 10.11%, respectively, compared to the days that occurred before the storm. The performance of the outdoor modules decreased by 16.89%, 8.7%, 33.66% and 35.19% for current, voltage, power and efficiency, respectively. From the weight of the dust accumulated on the PV modules, it was noted that its percentage was high for the days after the storm compared to the days before it. During a storm, it is futile to clean modules due to the high concentration of dust in the air. However, the modules can be dry cleaned with bristle brushes after a storm has subsided.

Author Contributions: Conceptualization, M.T.C. and H.A.K.; methodology, A.H.A.A.-W.; software, H.A.D.; validation, K.S. and H.A.D.; formal analysis, H.A.D. and M.A.F.; investigation, M.T.C. and W.H.A.; resources, A.A.A.-A.; data curation, W.N.R.W.I.; writing—original draft preparation, M.T.C.; writing—review and editing, A.A.A.-A.; visualization, W.N.R.W.I.; supervision, A.A.A.-A.; project administration, W.H.A.; funding acquisition, M.A.F. All authors have read and agreed to the published version of the manuscript.

Funding: This research received no external funding.

Data Availability Statement: Not applicable.

Acknowledgments: The authors extend their appreciation to the Universiti Kebangsaan Malaysia. The authors also extend their sincere thanks to all the staff at the Center of Advanced Research in Power Generation and Fuels (CAPF), School of Engineering and Design, Brunel University, London, UK. We also greatly appreciate Kenneth Antis, Lantern Christodoulou and David Pearce.

Conflicts of Interest: The authors declare no conflict of interest.

References

1. Böök, H.; Lindfors, A.V. Site-specific adjustment of a NWP-based photovoltaic production forecast. *Sol. Energy* **2020**, *211*, 779–788. [CrossRef]
2. REN21. *Renewables 2020 Global Status Report*; REN21 Secretariat: Paris, France, 2020.
3. Soret, A.; Piot, M.; Ortega, D.; Basart, S. Solar power forecasting: Application of the NMMB/BSC-CTM online chemical weather prediction model in central Europe. In Proceedings of the 16th EMS Annual Meeting & 11th European Conference on Applied Climatology (ECAC), Trieste, Italy, 11–16 September 2016.
4. Alwar, S.; Samithas, D.; Boominathan, M.S.; Balachandran, P.K.; Mihet-Popa, L. Performance Analysis of Thermal Image Processing-Based Photovoltaic Fault Detection and PV Array Reconfiguration—A Detailed Experimentation. *Energies* **2022**, *15*, 8450. [CrossRef]
5. Kazem, H.A.; Chaichan, M.T.; Alwaeli, A.H.; Mani, K. Effect of shadows on the performance of solar photovoltaic. In *Mediterranean Green Buildings & Renewable Energy*; Springer: Cham, Switzerland, 2017; pp. 379–385.
6. Ramli, M.A.M.; Prasetyono, E.; Wicaksana, R.W.; Windarko, N.A.; Sedraoui, K.; Al-Turki, Y.A. On the investigation of photovoltaic output power reduction due to dust accumulation and weather conditions. *Renew. Energy* **2016**, *99*, 836–844. [CrossRef]
7. Hammad, B.; Al-Abed, M.; Al-Ghandoor, A.; Al-Sardeah, A.; Al-Bashir, A. Modeling and analysis of dust and temperature effects on photovoltaic systems' performance and optimal cleaning frequency: Jordan case study. *Renew. Sustain. Energy Rev.* **2008**, *82*, 2218–2234. [CrossRef]
8. Chaichan, M.T.; Mohammed, B.A.; Kazem, H.A. Effect of pollution and cleaning on photovoltaic performance based on experimental study. *Int. J. Sci. Eng. Res.* **2015**, *6*, 594–601. [CrossRef]
9. Kazem, A.A.; Chaichan, M.T.; Kazem, H.A. Dust effect on photovoltaic utilization in Iraq: Review article. *Renew. Sustain. Energy Rev.* **2014**, *37*, 734–749. [CrossRef]
10. Sissakian, V.K.; Al-Ansari, N.; Knutsson, S. Sand and dust storm events in Iraq. *J. Nat. Sci.* **2013**, *5*, 1084–1094. [CrossRef]
11. Lee, J. Iraq Dust Storm Puts 5,000 in Hospital. *Iraq Business News*, 6 May 2022.
12. Iraq dust storm leaves 5,000 people needing treatment. *BBC News*, 5 May 2022.
13. Iraq dust storm hospitalizes 1,000 people and suspends flights. *The Independent*, 5 May 2022.
14. Iraq dust storm: Flights grounded in Baghdad and Najaf as skies turn orange. *BBC News*, 1 May 2022. (In English)
15. Iraq yet again hit by increasingly frequent dust storms. *France 24*, 1 May 2022. (In English)
16. Iraq records first death from weeks-long dust storm. *The New Arab*, 5 May 2022.
17. Dust Storms Choke Iraq. Available online: <https://al-ain.com/> (accessed on 16 May 2022).

18. Wang, N.; Zhang, Q.; Sun, S.; Wang, H.; He, M.; Zheng, P.; Wang, R. A sandstorm extreme event from the Yellow River Basin in March 2021: Accurate identification and driving cause. *Sci. Total Environ.* **2022**, *846*, 157424. [CrossRef]
19. Tanaka, T.Y.; Chiba, M. A numerical study of the contributions of dust source regions to the global dust budget. *Glob. Planet. Chang.* **2006**, *52*, 88–104. [CrossRef]
20. Huneus, N.; Schulz, M.; Balkanski, Y.; Griesfeller, J.; Prospero, J.; Kinne, S.; Bauer, S.; Boucher, O.; Chin, M.; Dentener, F.; et al. Global dust model intercomparison in AeroCom phase I. *Atmos. Chem. Phys.* **2011**, *11*, 7781–7816. [CrossRef]
21. Zhang, X.X.; Shi, P.J.; Liu, L.Y.; Tang, Y.; Cao, H.W.; Zhang, X.N.; Hu, X.; Guo, L.L.; Lue, Y.L.; Qu, Z.Q.; et al. Ambient TSP concentration and dust fall in major cities of China: Spatial distribution and temporal variability. *Atmos. Environ.* **2010**, *44*, 1641–1648. [CrossRef]
22. Middleton, N.J.; Goudie, A.S. Saharan dust: Sources and trajectories. *Trans. Inst. Br. Geogr.* **2001**, *26*, 165–181. [CrossRef]
23. Masson-Delmotte, V.; Zhai, P.; Pirani, A.; Connors, S.L.; Péan, C.; Berger, S.; Caud, N.; Chen, Y.; Goldfarb, L.; Gomis, M.I.; et al. *Climate Change 2021: The Physical Science Basis*; Contribution of Working Group I to the Sixth Assessment Report of the Intergovernmental Panel on Climate Change; IPCC: Geneva, Switzerland, 2021; Volume 2, Available online: <https://www.ipcc.ch/report/ar6/wg1/> (accessed on 16 May 2022).
24. Wang, N.X.; Sun, J.F.; Wei, B.; Mei, Q.; An, Z.X.; Wei, F.H.; Li, M.X.; Qiu, Z.X.; Bo, X.F.; Xie, J.; et al. Gaseous and heterogeneous reactions on the mechanisms and kinetics of acrolein with ozone. *Atmos. Environ.* **2021**, *254*, 118392. [CrossRef]
25. Luo, F. Analysis of Characteristics of Urban Atmospheric Pollution in Jinan City. In Proceedings of the 2010 4th International Conference on Bioinformatics and Biomedical Engineering (ICBBE 2010), Chengdu, China, 18–20 June 2010; p. 3.
26. Gu, Z.L.; He, Y.P.; Zhang, Y.W.; Su, J.W.; Zhang, R.J.; Yu, C.W.; Zhang, D.Z. An overview of triggering mechanisms and characteristics of local strong sandstorms in China and haboobs. *Atmosphere* **2021**, *12*, 17. [CrossRef]
27. Yang, S.; Duan, F.; Ma, Y.; Li, H.; Ma, T.; Zhu, L.; Huang, T.; Kimoto, T.; He, K. Mixed and intensive haze pollution during the transition period between autumn and winter in Beijing, China. *Sci. Total Environ.* **2020**, *711*, 134745. [CrossRef]
28. Luo, X.; Li, Y.; Li, Y.; Li, J.; Zhang, A. Research on relation between sandy weather in east of Hexi corridor and air pollution in Wuwei City. *J. Desert Res.* **2004**, *24*, 642–646.
29. Zhang, X.-Y.; Gong, S.L.; Shen, Z.X.; Mei, F.M.; Xi, X.X.; Liu, L.C.; Zhou, Z.J.; Wang, D.; Wang, Y.Q.; Cheng, Y. Characterization of soil dust aerosol in China and its transport and distribution during 2001 ACE-Asia: 1. Network observations. *J. Geophys. Res. Atmos.* **2003**, *108*, 13. [CrossRef]
30. Wang, N.; Wei, F.; Sun, J.; Wei, B.; Mei, Q.; An, Z.; Li, M.; Qiu, Z.; Bo, X.; Xie, J.; et al. Atmospheric ozonolysis of crotonaldehyde in the absence and presence of hydroxylated silica oligomer cluster adsorption. *Chemosphere* **2021**, *281*, 130996. [CrossRef]
31. Wang, N.X.; Zheng, P.M.; Wang, R.Q.; Wei, B.; An, Z.X.; Li, M.X.; Xie, J.; Wang, Z.M.; Wang, H.; He, M.X. Homogeneous and heterogeneous atmospheric ozonolysis of acrylonitrile on the mineral dust aerosols surface. *J. Environ. Chem. Eng.* **2021**, *9*, 10. [CrossRef]
32. Zhao, X.; Zhang, X.; Pu, W.; Meng, W.; Xu, X. Scattering properties of the atmospheric aerosol in Beijing, China. *Atmos. Res.* **2011**, *101*, 799–808. [CrossRef]
33. Garland, R.M.; Schmid, O.; Nowak, A.; Achtert, P.; Wiedensohler, A.; Gunthe, S.S.; Takegawa, N.; Kita, K.; Kondo, Y.; Hu, M.; et al. Aerosol optical properties observed during Campaign of Air Quality Research in Beijing 2006 (CAREBeijing-2006): Characteristic differences between the inflow and outflow of Beijing city air. *J. Geophys. Res. Atmos.* **2009**, *114*, D00G04. [CrossRef]
34. Maghrabi, A.H.; Al-Dosari, A.F. Effects on surface meteorological parameters and radiation levels of a heavy dust storm occurred in Central Arabian Peninsula. *Atmos. Res.* **2016**, *182*, 30–35. [CrossRef]
35. Al-Maamary, H.M.; Kazem, H.A.; Chaichan, M.T. Changing the energy profile of the GCC States: A review. *Int. J. Appl. Eng. Res.* **2016**, *11*, 1980–1988.
36. Al Shehhi, M.; Gherboudj, I.; Ghedira, H. An overview of historical harmful algae blooms outbreaks in the Arabian Seas. *Mar. Pollut. Bull.* **2014**, *86*, 314–324. [CrossRef] [PubMed]
37. Fryrear, D. Long-term effect of erosion and cropping on soil productivity. *Geol. Soc. Am.* **1981**, *186*, 253–260.
38. Javed, W.; Guo, B.; Figgis, B.; Pomares, L.M.; Aissa, B. Multi-year field assessment of seasonal variability of photovoltaic soiling and environmental factors in a desert environment. *Sol. Energy* **2020**, *211*, 1392–1402. [CrossRef]
39. Papi, R.; Attarchi, S.; Darvishi Bolorani, A.; Neysani Samany, N. Characterization of hydrologic sand and dust storm sources in the Middle East. *Sustainability* **2022**, *14*, 15352. [CrossRef]
40. Hagen, L.J.; Woodruff, N.P. Air pollution from dust storms in the Great Plains. *Atmos. Environ.* **1973**, *7*, 323–332. [CrossRef]
41. Zoljoodi, M.; Didevarasl, A.; Saadatabadi, A.R. Dust Events in the Western Parts of Iran and the Relationship with Drought Expansion over the Dust-Source Areas in Iraq and Syria. *Atmos. Clim. Sci.* **2013**, *03*, 321–336. [CrossRef]
42. Solomon, S.; Qin, D.; Manning, M.; Averyt, K.; Marquis, M. *Climate Change 2007—The Physical Science Basis*; Working Group I Contribution to the Fourth Assessment Report of the IPCC; Cambridge University Press: Cambridge, UK, 2007; Volume 4.
43. Dehshiri, S.S.H.; Firoozabadi, B.; Afshin, H. A new application of multi-criteria decision making in identifying critical dust sources and comparing three common receptor-based models. *Sci. Total Environ.* **2022**, *808*, 152109. [CrossRef]
44. Mostafaeipour, A.; Dehshiri, S.J.H.; Dehshiri, S.S.H. Ranking locations for producing hydrogen using geothermal energy in Afghanistan. *Int. J. Hydrogen Energy* **2020**, *45*, 15924–15940. [CrossRef]

45. Geravandi, S.; Sicard, P.; Khaniabadi, Y.O.; De Marco, A.; Ghomeishi, A.; Goudarzi, G.; Mahboubi, M.; Yari, A.R.; Dobaradaran, S.; Hassani, G.; et al. A comparative study of hospital admissions for respiratory diseases during normal and dusty days in Iran. *Environ. Sci. Pollut. Res.* **2017**, *24*, 18152–18159. [[CrossRef](#)]
46. Tezangi, M.F. Studying the role of climatic phenomena in road accidents in Yazd Province. *IIOAB J.* **2016**, *7*, 459–465.
47. Gholami, A.; Ameri, M.; Zandi, M.; Ghoachani, R.G.; Eslami, S.; Pierfederici, S. Photovoltaic Potential Assessment and Dust Impacts on Photovoltaic Systems in Iran: Review Paper. *IEEE J. Photovolt.* **2020**, *10*, 824–837. [[CrossRef](#)]
48. Shubbar, R.M.; Salman, H.H.; Lee, D.-I. Characteristics of climate variation indices in Iraq using a statistical factor analysis. *Int. J. Clim.* **2016**, *37*, 918–927. [[CrossRef](#)]
49. Kazem, H.A.; Chaichan, M.T.; Al-Waeli, A.H.; Sopian, K. Effect of dust and cleaning methods on mono and polycrystalline solar photovoltaic performance: An indoor experimental study. *Sol. Energy* **2022**, *236*, 626–643. [[CrossRef](#)]
50. Awadh, S.M. Impact of North African sand and dust storms on the Middle East using Iraq as an example: Causes, sources, and mitigation. *Atmosphere* **2023**, *14*, 180. [[CrossRef](#)]
51. Filonchik, M. Characteristics of the severe March 2021 Gobi Desert dust storm and its impact on air pollution in China. *Chemosphere* **2022**, *287*, 132219. [[CrossRef](#)] [[PubMed](#)]
52. Farahani, V.J.; Arhami, M. Contribution of Iraqi and Syrian dust storms on particulate matter concentration during a dust storm episode in receptor cities: Case study of Tehran. *Atmos. Environ.* **2020**, *222*, 117163. [[CrossRef](#)]
53. Francis, D.B.K.; Flamant, C.; Chaboureaud, J.-P.; Banks, J.; Cuesta, J.; Brindley, H.; Oolman, L. Dust emission and transport over Iraq associated with the summer Shamal winds. *Aeolian Res.* **2017**, *24*, 15–31. [[CrossRef](#)]
54. Vishkaee, F.A.; Flamant, C.; Cuesta, J.; Oolman, L.; Flamant, P.; Khalesifard, H.R. Dust transport over Iraq and northwest Iran associated with winter Shamal: A case study. *J. Geophys. Res. Atmos.* **2012**, *117*, D03201. [[CrossRef](#)]
55. Al Ameri, I.D.S.; Briant, R.M.; Engels, S. Drought severity and increased dust storm frequency in the Middle East: A case study from the Tigris-Euphrates alluvial plain, central Iraq. *Weather* **2019**, *74*, 416–426. [[CrossRef](#)]
56. Sarver, T.; Al-Qaraghuli, A.; Kazmerski, L.L. A comprehensive review of the impact of dust on the use of solar energy: History, investigations, results, literature, and mitigation approaches. *Renew. Sustain. Energy Rev.* **2013**, *22*, 698–733. [[CrossRef](#)]
57. Cai, W.; Li, X.; Maleki, A.; Pourfayaz, F.; Rosen, M.A.; Nazari, M.A.; Bui, D.T. Optimal sizing and location based on economic parameters for an off-grid application of a hybrid system with photovoltaic, battery and diesel technology. *Energy* **2020**, *201*, 117480. [[CrossRef](#)]
58. Ghenai, C.; Salameh, T.; Merabet, A. Technico-economic analysis of off grid solar PV/Fuel cell energy system for a residential community in desert region. *Int. J. Hydrogen Energy* **2020**, *45*, 11460–11470. [[CrossRef](#)]
59. Ram, M.; Aghahosseini, A.; Breyer, C. Job creation during the global energy transition towards 100% renewable power system by 2050. *Technol. Forecast. Soc. Chang.* **2020**, *151*, 119682. [[CrossRef](#)]
60. Andreani, L.C.; Bozzola, A.; Kowalczewski, P.; Liscidini, M.; Redorici, L. Silicon solar cells: Toward the efficiency limits. *Adv. Phys. X* **2019**, *4*, 1548305. [[CrossRef](#)]
61. Yao, W.; Han, X.; Huang, Y.; Zheng, Z.; Wang, Y.; Wang, X. Analysis of the influencing factors of the dust on the surface of photovoltaic panels and its weakening law to solar radiation—A case study of Tianjin. *Energy* **2022**, *256*, 124669. [[CrossRef](#)]
62. El Baqqal, Y.; Laarabi, B.; Dahrouch, A.; Barhdadi, A. Assessment of soiling effect on PV module glass transmittance in Moroccan capital region. *Environ. Sci. Pollut. Res.* **2020**, *27*, 44510–44518. [[CrossRef](#)]
63. Kazem, H.A.; Chaichan, M.T.; Al-Waeli, A.H.; Al-Badi, R.; Fayad, M.A.; Gholami, A. Dust impact on photovoltaic/thermal system in harsh weather conditions. *Sol. Energy* **2022**, *245*, 308–321. [[CrossRef](#)]
64. Gupta, V.; Sharma, M.; Pachauri, R.K.; Babu, K.N.D. Comprehensive review on effect of dust on solar photovoltaic system and mitigation techniques. *Sol. Energy* **2019**, *191*, 596–622. [[CrossRef](#)]
65. Ma, M.; Liu, H.; Zhang, Z.; Yun, P.; Liu, F. Rapid diagnosis of hot spot failure of crystalline silicon PV module based on IV curve. *Microelectron. Reliab.* **2019**, *100*, 113402. [[CrossRef](#)]
66. Mohammed, H.; Kumar, M.; Gupta, R. Bypass diode effect on temperature distribution in crystalline silicon photovoltaic module under partial shading. *Sol. Energy* **2020**, *208*, 182–194. [[CrossRef](#)]
67. Chanchangi, Y.N.; Ghosh, A.; Sundaram, S.; Mallick, T.K. Dust and PV Performance in Nigeria: A review. *Renew. Sustain. Energy Rev.* **2020**, *121*, 109704. [[CrossRef](#)]
68. Alnasser, T.M.; Mahdy, A.M.; Abass, K.I.; Chaichan, M.T.; Kazem, H.A. Impact of dust ingredient on photovoltaic performance: An experimental study. *Sol. Energy* **2020**, *195*, 651–659. [[CrossRef](#)]
69. Chaichan, M.T.; Kazem, H.A.; Al-Waeli, A.H.; Sopian, K. The effect of dust components and contaminants on the performance of photovoltaic for the four regions in Iraq: A practical study. *Renew. Energy Environ. Sustain.* **2020**, *5*, 3. [[CrossRef](#)]
70. Ilse, K.; Micheli, L.; Figgis, B.W.; Lange, K.; Daßler, D.; Hanifi, H.; Wolfertstetter, F.; Naumann, V.; Hagedorf, C.; Gottschalg, R.; et al. Techno-Economic Assessment of Soiling Losses and Mitigation Strategies for Solar Power Generation. *Joule* **2019**, *3*, 2303–2321. [[CrossRef](#)]
71. Costa, S.C.; Diniz, A.S.A.; Kazmerski, L.L. Dust and soiling issues and impacts relating to solar energy systems: Literature review update for 2012–2015. *Renew. Sustain. Energy Rev.* **2016**, *63*, 33–61. [[CrossRef](#)]
72. Ilse, K.K.; Figgis, B.W.; Werner, M.; Naumann, V.; Hagedorf, C.; Pöllmann, H.; Bagdahn, J. Comprehensive analysis of soiling and cementation processes on PV modules in Qatar. *Sol. Energy Mater. Sol. Cells* **2018**, *186*, 309–323. [[CrossRef](#)]

73. Zaihidee, F.M.; Mekhilef, S.; Seyedmahmoudian, M.; Horan, B. Dust as an unalterable deteriorative factor affecting PV panel's efficiency: Why and how. *Renew. Sustain. Energy Rev.* **2016**, *65*, 1267–1278. [[CrossRef](#)]
74. Alnaser, N.; Al Othman, M.; Dakhel, A.; Batarseh, I.; Lee, J.; Najmaii, S.; Alothman, A.; Al Shawaikh, H.; Alnaser, W. Comparison between performance of man-made and naturally cleaned PV panels in a middle of a desert. *Renew. Sustain. Energy Rev.* **2018**, *82*, 1048–1055. [[CrossRef](#)]
75. Sidiki, A.; Li, W.; Alhousseini, M. Experimental Evaluation of the Effect of Inclination and Dust Deposition on Production Capacity of Photovoltaic Installations in West African Nations: Case Study in Mali Drame. *Iran. J. Energy Environ.* **2018**, *9*, 91–99. [[CrossRef](#)]
76. Willoughby, A.A.; Osinowo, M.O. Development of an electronic load I-V curve tracer to investigate the impact of Harmattan aerosol loading on PV module performance in southwest Nigeria. *Sol. Energy* **2018**, *166*, 171–180. [[CrossRef](#)]
77. Hadwan, M.; Alkholidi, A. Assessment of factors influencing the sustainable performance of photovoltaic water pumping systems. *Renew. Sustain. Energy Rev.* **2018**, *92*, 307–318. [[CrossRef](#)]
78. Gholami, A.; Khazaei, I.; Eslami, S.; Zandi, M.; Akrami, E. Experimental investigation of dust deposition effects on photo-voltaic output performance. *Sol. Energy* **2018**, *159*, 346–352. [[CrossRef](#)]
79. Hammoud, M.; Shokr, B.; Assi, A.; Hallal, J.; Khoury, P. Effect of dust cleaning on the enhancement of the power generation of a coastal PV-power plant at Zahrani Lebanon. *Sol. Energy* **2019**, *184*, 195–201. [[CrossRef](#)]
80. Kazem, H.A.; Chaichan, M.T. The effect of dust accumulation and cleaning methods on PV panels' outcomes based on an experimental study of six locations in Northern Oman. *Sol. Energy* **2019**, *187*, 30–38. [[CrossRef](#)]
81. Al-Kouz, W.; Al-Dahidi, S.; Hammad, B.; Al-Abed, M. Modeling and Analysis Framework for Investigating the Impact of Dust and Temperature on PV Systems' Performance and Optimum Cleaning Frequency. *Appl. Sci.* **2019**, *9*, 1397. [[CrossRef](#)]
82. Salamah, T.; Ramahi, A.; Alamara, K.; Juaidi, A.; Abdallah, R.; Abdelkareem, M.A.; Amer, E.C.; Olabi, A.G. Effect of dust and methods of cleaning on the performance of solar PV module for different climate regions: Comprehensive review. *Sci. Total Environ.* **2022**, *827*, 154050. [[CrossRef](#)]
83. Alquthami, T.; Menoufi, K. Soiling of Photovoltaic Modules: Comparing between Two Distinct Locations within the Framework of Developing the Photovoltaic Soiling Index (PVSI). *Sustainability* **2019**, *11*, 4697. [[CrossRef](#)]
84. Al-Housani, M.; Bicer, Y.; Koç, M. Assessment of various dry photovoltaic cleaning techniques and frequencies on the power output of CdTe-type modules in dusty environments. *Sustainability* **2019**, *11*, 2850. [[CrossRef](#)]
85. Quansah, D.A.; Adaramola, M.S. Assessment of early degradation and performance loss in five co-located solar photovoltaic module technologies installed in Ghana using performance ratio time-series regression. *Renew. Energy* **2019**, *131*, 900–910. [[CrossRef](#)]
86. Alawasa, K.; Alabri, R.; Al-Hinai, A.; Albadi, M.; Al-Badi, A. Experimental Study on the Effect of Dust Deposition on a Car Park Photovoltaic System with Different Cleaning Cycles. *Sustainability* **2021**, *13*, 7636. [[CrossRef](#)]
87. Salimi, H.; Mirabdollah Lavasani, A.; Ahmadi-Danesh-Ashtiani, H.; Fazaeli, R. Effect of dust concentration, wind speed, and relative humidity on the performance of photovoltaic panels in Tehran. *Energy Sources Part A Recover. Util. Environ. Eff.* **2019**, *1–11*. [[CrossRef](#)]
88. Lu, H.; Cai, R.; Zhang, L.-Z.; Lu, L.; Zhang, L. Experimental investigation on deposition reduction of different types of dust on solar PV cells by self-cleaning coatings. *Sol. Energy* **2020**, *206*, 365–373. [[CrossRef](#)]
89. Al-Badra, M.; Abd-Elhady, M.; Kandil, H. A novel technique for cleaning PV panels using antistatic coating with a mechanical vibrator. *Energy Rep.* **2020**, *6*, 1633–1637. [[CrossRef](#)]
90. Ullah, A.; Amin, A.; Haider, T.; Saleem, M.; Butt, N.Z. Investigation of soiling effects, dust chemistry and optimum cleaning schedule for PV modules in Lahore, Pakistan. *Renew. Energy* **2020**, *150*, 456–468. [[CrossRef](#)]
91. Kazem, H.A.; Chaichan, M.T.; Al-Waeli, A.H.; Sopian, K. Evaluation of aging and performance of grid-connected photovoltaic system northern Oman: Seven years' experimental study. *Sol. Energy* **2020**, *207*, 1247–1258. [[CrossRef](#)]
92. Majeed, R.; Waqas, A.; Sami, H.; Ali, M.; Shahzad, N. Experimental investigation of soiling losses and a novel cost-effective cleaning system for PV modules. *Sol. Energy* **2020**, *201*, 298–306. [[CrossRef](#)]
93. Semaoui, S.; Abdeladim, K.; Taghezouit, B.; Arab, A.H.; Razagui, A.; Bacha, S.; Boulahchiche, S.; Bouacha, S.; Gherbi, A. Experimental investigation of soiling impact on grid connected PV power. *Energy Rep.* **2020**, *6*, 302–308. [[CrossRef](#)]
94. Mustafa, R.J.; Gomaa, M.R.; Al-dhaifallah, M.; Rezk, H. Environmental impacts on the performance of solar photovoltaic systems. *Sustainability* **2020**, *12*, 608. [[CrossRef](#)]
95. Darwish, Z.A.; Sopian, K.; Fudholi, A. Reduced output of photovoltaic modules due to different types of dust particles. *J. Clean. Prod.* **2021**, *280*, 124317. [[CrossRef](#)]
96. Al Bakri, H.; Abu Elhajja, W.; Al Zyoud, A. Solar photovoltaic panels performance improvement using active self-cleaning nanotechnology of SurfaShield, G. *Energy* **2021**, *223*, 119908. [[CrossRef](#)]
97. Yazdani, H.; Yaghoubi, M. Techno-economic study of photovoltaic systems performance in Shiraz, Iran. *Renew. Energy* **2021**, *172*, 251–262. [[CrossRef](#)]
98. Kennedy, J.; Lo, A.; Rajamani, H.-S.; Lutfi, S. Solar and sand: Dust deposit mitigation in the desert for PV arrays. *Sustain. Energy Grids Netw.* **2021**, *28*, 100531. [[CrossRef](#)]
99. Lasfar, S.; Haidara, F.; Mayouf, C.; Abdellahi, F.M.; Elghorba, M.; Wahid, A.; Kane, C.S.E. Study of the influence of dust deposits on photovoltaic solar panels: Case of Nouakchott. *Energy Sustain. Dev.* **2021**, *63*, 7–15. [[CrossRef](#)]

100. Hamid, R.H.A.; Elidrissi, Y.; Elsamahy, A.; Regragui, M.; Menoufi, K. Examining the Impact of Different Technical and Environmental Parameters on the Performance of Photovoltaic Modules. *Environ. Clim. Technol.* **2021**, *25*, 1–11. [[CrossRef](#)]
101. Zeedan, A.; Barakeh, A.; Al-Fakhroo, K.; Touati, F.; Gonzales, A.S., Jr. Quantification of PV power and economic losses due to soiling in Qatar. *Sustainability* **2021**, *13*, 3364. [[CrossRef](#)]
102. Kazem, H.A.; Chaichan, M.T.; Al-Waeli, A.H. A comparison of dust impacts on polycrystalline and monocrystalline solar photovoltaic performance: An outdoor experimental study. *Environ. Sci. Pollut. Res.* **2022**, *29*, 88788–88802. [[CrossRef](#)]
103. Şevik, S.; Aktaş, A. Performance enhancing and improvement studies in a 600 kW solar photovoltaic (PV) power plant; manual and natural cleaning, rainwater harvesting and the snow load removal on the PV arrays. *Renew. Energy* **2022**, *181*, 490–503. [[CrossRef](#)]
104. Yazdani, H.; Yaghoubi, M. Dust deposition effect on photovoltaic modules performance and optimization of cleaning period: A combined experimental-numerical study. *Sustain. Energy Technol. Assess.* **2022**, *51*, 101946. [[CrossRef](#)]
105. Enaganti, P.K.; Bhattacharjee, A.; Ghosh, A.; Chanchangi, Y.N.; Chakraborty, C.; Mallick, T.K.; Goel, S. Experimental investigations for dust build-up on low-iron glass exterior and its effects on the performance of solar PV systems. *Energy* **2022**, *239*, 122213. [[CrossRef](#)]
106. Juaidi, A.; Muhammad, H.H.; Abdallah, R.; Abdalhaq, R.; Albatayneh, A.; Kawa, F. Experimental validation of dust impact on-grid connected PV system performance in Palestine: An energy nexus perspective. *Energy Nexus* **2022**, *6*, 100082. [[CrossRef](#)]
107. Abdulazeez, Z.M. Experimental Investigation of the Effect of Dust on Monocrystalline Photovoltaic Module Performance in Kirkuk, Iraq. *Kirkuk Univ. J. Sci. Stud.* **2018**, *13*, 127–138. [[CrossRef](#)]
108. Hameed, H.G.; Hachim, D.M.; Al-Hilo, A.S.; Mazen, A.; Ali, L.; Maqdad, N.; Farhan, Z. Study the effect of dust on performance of PV panel and design cleaning system. *Int. J. Energy Environ.* **2019**, *10*, 119–126.
109. Jassim, A.H.; Abed, F.M.; Mohamed, M.A. The effect of atmospheric dust accumulation on the performance of the hybrid solar collector in the semi-arid regions of Iraq. *Des. Eng.* **2021**, *8*, 3934–3948.
110. Abbas, E.F. Determining the Impact of the Environmental Condition on the Production Performance of Photovoltaic in Kirkuk, Iraq. *New Approaches Eng. Res.* **2021**, *12*, 121–132. [[CrossRef](#)]
111. Chaichan, M.T.; Kazem, H.A. Experimental evaluation of dust composition impact on photovoltaic performance in Iraq. *Energy Sources Part A Recovery Util. Environ. Eff.* **2020**, 1–22. [[CrossRef](#)]
112. Mahmood, A.L.; Shakir, A.M.; Numan, B.A. Design and performance analysis of stand-alone PV system at Al-Nahrain University, Baghdad, Iraq. *Int. J. Power Electron. Drive Syst. IJPEDS* **2020**, *11*, 921–930. [[CrossRef](#)]
113. Kasim, N.K.; Obaid, N.M.; Abood, H.G.; Mahdi, R.A.; Humada, A.M. Experimental study for the effect of dust cleaning on the performance of grid-tied photovoltaic solar systems. *Int. J. Electr. Comput. Eng. IJECE* **2021**, *11*, 74–83. [[CrossRef](#)]
114. Aghahosseini, A.; Bogdanov, D.; Ghorbani, N.; Breyer, C. Analysis of 100% renewable energy for Iran in 2030: Integrating solar PV, wind energy and storage. *Int. J. Environ. Sci. Technol.* **2018**, *15*, 17–36. [[CrossRef](#)]
115. Chaichan, M.T.; Kazem, H.A. *Generating Electricity Using Photovoltaic Solar Plants in Iraq*; Springer: Berlin/Heidelberg, Germany, 2018; pp. 47–82.
116. Holman, J.P. *Experimental Methods for Engineers*; McGraw-Hill: New York, NY, USA, 2012.
117. Al-Waeli, A.H.; Chaichan, M.T.; Kazem, H.A.; Sopian, K.; Ibrahim, A.; Mat, S.; Ruslan, M.H. Comparison study of indoor/outdoor experiments of a photovoltaic thermal PV/T system containing SiC nanofluid as a coolant. *Energy* **2018**, *151*, 33–44. [[CrossRef](#)]
118. Al-Waeli, A.H.; Sopian, K.; Kazem, H.A.; Chaichan, M.T. Photovoltaic/Thermal (PV/T) systems: Status and future prospects. *Renew. Sustain. Energy Rev.* **2017**, *77*, 109–130. [[CrossRef](#)]
119. Hamza, N.H.; Ekaab, N.S.; Chaichan, M.T. Impact of using Iraqi biofuel–kerosene blends on coarse and fine particulate matter emitted from compression ignition engines. *Alex. Eng. J.* **2020**, *59*, 1717–1724. [[CrossRef](#)]

Disclaimer/Publisher’s Note: The statements, opinions and data contained in all publications are solely those of the individual author(s) and contributor(s) and not of MDPI and/or the editor(s). MDPI and/or the editor(s) disclaim responsibility for any injury to people or property resulting from any ideas, methods, instructions or products referred to in the content.